Journal of Glaciology



Article

Cite this article: Eswaran A, Truax OJ, MacDonell S, Matsuoka K, Neff PD, Steig EJ, Winton VHL and Fudge TJ (2026) Data-driven optimization of Antarctic shallow ice core site selection. *Journal of Glaciology* **72**, e102, 1–20. https://doi.org/10.1017/jog.2026.10218

Received: 20 September 2025 UTC
Revised: 10 September 2026 UTC
Accepted: 12 September 2026 UTC

Keywords:
accumulation; ice and climate; ice core; ice coring; paleoclimate

Corresponding author: Advik Eswaran;
Email: advike@princeton.edu

© The Author(s), 2026. Published by Cambridge University Press on behalf of International Glaciological Society. This is an Open Access article, distributed under the terms of the Creative Commons Attribution licence (http://creativecommons.org/licenses/by/4.0), which permits unrestricted re-use, distribution and reproduction, provided the original article is properly cited.

cambridge.org/jog

Data-driven optimization of Antarctic shallow ice core site selection

Advik Eswaran[1], Olivia J. Truax[2,3], Shelley MacDonell[2], Kenichi Matsuoka[4], Peter D. Neff[5], Eric J. Steig[3], V. Holly L. Winton[6] and T. J. Fudge[3]

[1]Department of Geosciences, Princeton University, Princeton, New Jersey, USA; [2]Te Kura Aronukurangi School of Earth and Environment, University of Canterbury, Christchurch, New Zealand; [3]Department of Earth and Space Sciences, University of Washington, Seattle, Washington, USA; [4]Norwegian Polar Institute, Tromsø, Norway; [5]Department of Soil, Water, and Climate, University of Minnesota, St. Paul, Minnesota, USA and [6]Antarctic Research Center, Victoria University of Wellington, Wellington, New Zealand

Abstract

Antarctic ice cores provide highly detailed climate histories; yet, the existing proxy record is limited by uneven spatial and temporal coverage. Collecting new ice cores will improve our understanding of climate processes in Antarctica, but the cost of drilling new records demands careful site selection. Here, we present a data-driven optimal sensor approach to select ice core sites that best constrain a chosen climate metric by iteratively applying an Ensemble Kalman Filter. We demonstrate the method by choosing two Antarctic-wide metrics: average annually resolved temperature and annual accumulation since the Industrial Era. Our approach accounts for proxy uncertainty based on the site accumulation rate; we discuss logistical constraints for specific case studies. We find that the southern Ross Ice Shelf and western Dronning Maud Land are optimal regions to reconstruct Antarctic-wide total accumulation and average temperature, respectively. We describe three case studies: 1) drilling a new core at Crary Ice Rise on the Ross Ice Shelf; 2) drilling a new core at Lyddan Ice Rise in Dronning Maud Land; and 3) redrilling the US-ITASE cores in West Antarctica. Our data-driven methodology can guide future community drilling efforts to maximize the value of new ice cores for climate reconstruction.

1. Introduction

The future contribution of Antarctica to sea level rise is uncertain, with models disagreeing on the sign of the contribution over the next century (Edwards and others, 2021; Payne and others, 2021; Seroussi and others, 2024). Similarly, early 21st-century observations find that Antarctica can gain (Smith and others, 2020) or lose (Rignot and others, 2019; Velicogna and others, 2020) mass depending on the time period studied. Gains in ice sheet mass from increased snowfall can mitigate the sea level contribution due to dynamic ice loss (Medley and Thomas, 2019). The combination of spatial and temporal variability can have compounding impacts on estimating Antarctic-wide climate averages. While climate models project snowfall to increase as a response to warming temperatures (Frieler and others, 2015; Lenaerts and others, 2016), empirical studies indicate high uncertainty in the sensitivity of accumulation to temperature (Monnin and others, 2004; Fudge and others, 2016; Nicola and others, 2023). Satellite observations indicate that the ice sheet has gained mass since 2020 due to increased snowfall from East Antarctica (Wang and others, 2025), but long-term dynamic ice loss is also projected to continue and likely increase (O'Neill and others, 2025). Similar uncertainty surrounds the historical variability of Antarctic temperature, which is important to constrain the sensitivity of Antarctic climate to natural and anthropogenic forcings (Stenni and others, 2017).

Understanding modern climate change in Antarctica is challenging due to a deficiency of reliable observations. The number of Antarctic weather stations is limited (Hakim and others, 2020), satellite observations for gravimetry and altimetry only span recent decades (e.g. Rignot and others, 2019), and instrumental reanalyses are reliable only since the beginning of the satellite era (i.e. 1979; Schneider and Fogt, 2018) and have significant limitations in accuracy (e.g. Dale and others, 2017; Bromwich and others, 2024). A greater understanding of past trends is necessary to place modern changes in Antarctic accumulation and temperature variability in a historical context. Ice core records offer a means to reconstruct Antarctic climate variability (e.g. Kaspari and others, 2004; Monaghan and others, 2006; Schneider and others, 2006; Goosse and others, 2012; Steig and others, 2013; Steiger and others, 2017).

The spatial distribution of annually resolved ice core records across the Antarctic Ice Sheet (AIS) is uneven (Fig. 1a); there is a relatively high density of cores located on the West Antarctic Ice Sheet (WAIS) and Antarctic Peninsula and a relative sparsity on the East Antarctic Ice Sheet

Downloaded from https://www.cambridge.org/core. 15 Nov 2026 at 21:07:29, subject to the Cambridge Core terms of use.

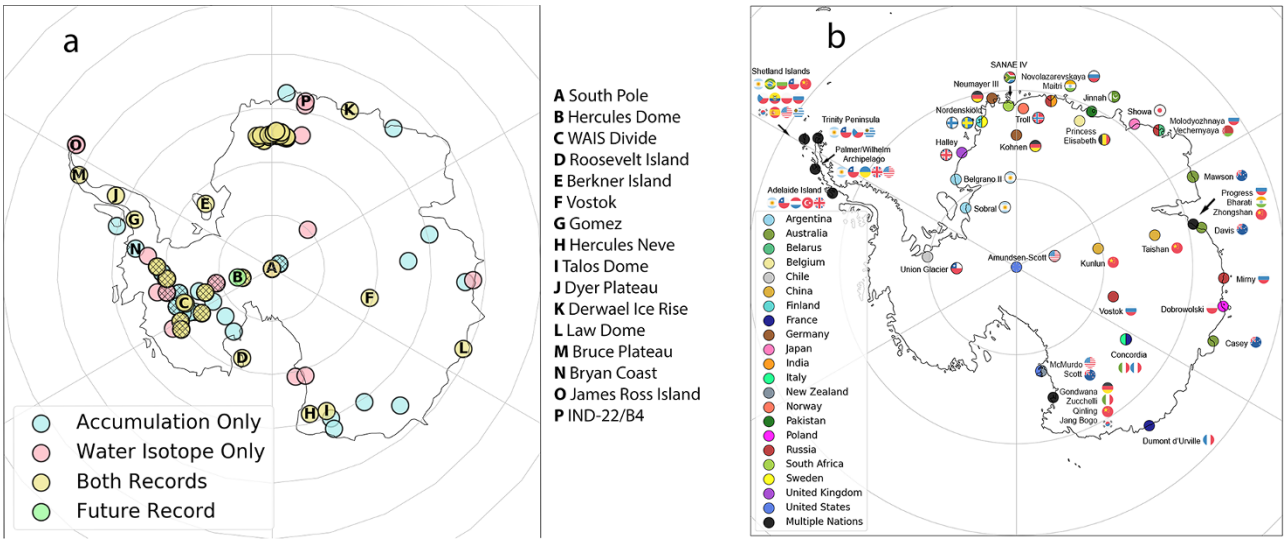


Figure 1. (a) Locations of 110 existing annually resolved ice core accumulation and water isotope records across the Antarctic Ice Sheet (Stenni and others, 2017; Thomas and others, 2017). (b) Locations of national research bases in Antarctica. Cores drilled as part of the US component of the ITASE program (Steig and others, 2013) are indicated in (a) with cross-hatching.

(EAIS). Low accumulation rates across the interior EAIS often preclude accurate annual dating and necessitate drilling in coastal areas, which are often more logistically and topographically complex (Vance and others, 2016). The resulting uncertainty in the EAIS proxy record may limit our ability to quantify both historical Antarctic temperature variability and sea level contribution (Klein and others, 2019; Medley and Thomas, 2019; Wang and Xiao, 2023; Eswaran and others, 2024). The EAIS is the largest contributor to Antarctic surface mass balance (Mottram and others, 2021), and future changes in EAIS mass are a major source of uncertainty in projections of future sea level rise (Seroussi and others, 2024). In addition to spatial limitations in the ice core record, there are also temporal limitations; the majority of Antarctic ice cores were drilled in the 1990s and 2000s, and fewer records cover the 21st century than any other time period since 1800 CE (Stenni and others, 2017; Thomas and others, 2017). This limits our ability to place 21st-century Antarctic climate variability in a historical context, and to understand spatial variability by comparing ice core records with modern surface and satellite observations.

Ice cores have often been drilled to reconstruct local and regional climate signals (e.g. Curran and others, 1998; Criscitiello and others, 2013; Philippe and others, 2016; Thomas and Abram, 2016). Vance and others (2016) provide a detailed description of many of the factors typically evaluated when selecting a site, targeting a regional rather than continental-scale signal. For the Mount Brown South ice core, Vance and others (2016) assess the glaciological characteristics (accumulation rate, timescale, windborne redistribution of snow and ice-flow velocity) and atmospheric circulation criteria (strong mid-latitude teleconnection and complementary relationship to other ice cores) focused on the Indo-Pacific. One challenge of climate reconstructions is how to extract a continental-scale signal from the noisy and conflicting regional signals. The PAGES Antarctica 2k working group has compiled annually resolved ice core-based reconstructions of Antarctic accumulation (Thomas and others, 2017) and temperature (Stenni and others, 2017) for the past 1000 years. They create regional composites for seven different Antarctic regions, which are then spatially averaged into a single continental-scale reconstruction. Accumulation and temperature trends vary greatly between regions; for example, snow accumulation is increasing in the Antarctic Peninsula but decreasing in Dronning Maud Land (DML) (Thomas and others, 2017), and the Antarctic Peninsula and West Antarctica are warming while the East Antarctic Plateau shows little significant warming (Steig and others, 2009; Stenni and others, 2017). In this paper, we seek an answer to the question: where should new ice core records be collected to maximize the potential continental-scale information gain?

Here, we present an objective, data-driven method for selecting shallow ice core drilling sites (spanning the past ~200 years) to optimize reconstruction of any climate metric of interest at annual resolution. Our paper presents an optimization of two climate metrics: annual snow accumulation (ice equivalent) and average annual surface air temperature. These metrics were chosen to follow the PAGES Antarctica 2k studies (Stenni and others, 2017; Thomas and others, 2017), and are taken as spatially integrated across the entire AIS, as well as WAIS and EAIS separately. Increased snow accumulation over Antarctica has a mitigating effect on sea level rise; spatially-integrated accumulation quantifies the extent of this sea level mitigation, which constrains the contribution of the AIS to past sea level change (Medley and Thomas, 2019). Average Antarctic surface air temperature can constrain the Antarctic temperature-accumulation relationship by quantifying the Clausius-Clapeyron sensitivity (Nicola and others, 2023). More generally, it constrains the response of Antarctic climate to natural and anthropogenic forcings (Stenni and others, 2017), such as climate sensitivity to CO_2 (e.g. Uemura and others, 2018). We use the terms 'annual Antarctic accumulation' and 'annual Antarctic temperature' moving forward to refer to these metrics.

We use an optimal sensor analysis, an established technique that has gained increasing use in paleoclimatology and meteorology for improving the selection of observational sites. Previous studies have performed optimal sensor analyses to evaluate and design networks of weather stations in the Pacific Northwest (Mauger and others, 2013) and Antarctica (Bumbaco and others, 2014; Hakim and others, 2020), as well as coral $\delta^{18}O$ proxy records (Comboul and others, 2015). An equivalent analysis does not exist for the

Downloaded from https://www.cambridge.org/core. 15 Nov 2026 at 21:07:29, subject to the Cambridge Core terms of use.

Antarctic ice core proxy network. We use the ensemble Kalman filter-based optimal sensor methodology implemented by King and others (2023a), which follows that of Comboul and others (2015). We additionally consider the physical and logistical constraints that are critical for any rigorous evaluation of potential ice core drilling sites (e.g. Vance and others, 2016). We emphasize that our methodology is generalizable to any climate metric. The underlying method can be used to optimize ice core site selection for a broad array of research questions, including different climate variables and smaller spatial scales.

We evaluate optimal Antarctic ice core drilling locations to reconstruct annual Antarctic accumulation and annual Antarctic temperature from 1801 to 2000 CE. To do so, we evaluate the statistical covariance and variance relationships from two different climate ensembles, which are constructed with either nine CMIP5 Last Millennium simulations or four instrumental reanalyses. We also account for proxy uncertainty by weighting against low-accumulation locations. An efficient search algorithm (Comboul and others, 2015; King and others, 2023a) allows us to incorporate this information into a quantitative optimal ranking of potential ice core sites. We then qualitatively consider physical and logistical factors, such as ice flow and topography, to ground our analysis with real-world constraints.

2. Methods

2.1 Methods overview

We treat ice core site selection as an optimal sensor problem, where we utilize the ensemble Kalman filter-based algorithm implemented by King and others (2023a), which follows that of Comboul and others (2015). This method iteratively designs an optimal Antarctic ice core proxy network by ranking the ability of potential proxy sites to constrain the variance of a given climate metric sampled across an ensemble of climate estimates.

The optimal sensor algorithm requires three inputs:

1) the climate metric to be reconstructed
2) the proxy estimates representing each potential ice core location
3) the proxy uncertainty for each proxy estimate

The climate metric and proxy estimates are sourced from either an ensemble of CMIP5 simulations or an ensemble of instrumental reanalyses. Metrics are calculated as spatially-integrated averages across either AIS, WAIS or EAIS. The proxy uncertainty is estimated by scaling with the inverse of accumulation rate (more detail in 2.5). The following sections explain these methods in further detail.

We run three different experiments.

1) The 'blank slate' experiment designs an optimal ice core network from scratch (i.e., assuming no ice core records exist).
2) The 'augmented network' experiment incorporates information from existing ice cores and finds sites to complement the existing network.
3) The 'redrilling' experiment finds which existing ice cores would provide the greatest information gain with an extension to the present, drawing only from existing ice core sites.

2.2 Optimal sensor algorithm

The optimal sensor algorithm iteratively uses an ensemble Kalman filter and an ensemble of climate simulations to rank potential proxy data sites.

Given n potential proxy records (potential ice core sites) and m ensemble members, the algorithm requires three inputs:

1) Climate metric: $\mathbf{J}$ is the climate metric we wish to reconstruct. For our experiments, it is either annual Antarctic accumulation or average annual Antarctic temperature. J is a scalar metric distributed across m ensemble members ($1 \times m$ row vector).
2) Proxy estimates: $\hat{\mathbf{Y}}$ is the synthetic proxy estimates, which are designed to simulate hypothetical accumulation or $\delta^{18}O$ records from all grid cells across Antarctica. $\hat{\mathbf{Y}}$ is the proxy estimates for n proxy sites, distributed across m ensemble members ($n \times m$ matrix)
3) Proxy uncertainties: $\mathbf{R}$ is the uncertainty assigned to each hypothetical ice core record, and scales inversely with accumulation rate. $\mathbf{R}$ is the estimated uncertainty in each of n proxy records ($n \times n$ diagonal matrix)

A $n \times 1$ vector $\mathbf{\Delta\sigma}$ is computed according to the following equation:

$$\mathbf{\Delta}\sigma_{\mathbf{i}} = \mathbf{cov}(\hat{\mathbf{Y}}_{\mathbf{i}}, \mathbf{J})^2 \left[\mathbf{var}\left(\hat{\mathbf{Y}}_{\mathbf{i}}\right) + \mathbf{R}_{\mathbf{ii}}\right]^{-1} \quad (1)$$

where the scalar $\mathbf{\Delta\sigma_i}$ is the amount of variance in $\mathbf{J}$ that can be reduced by the $\mathbf{i}$th proxy record.

The proxy $\hat{\mathbf{Y}}_{\mathbf{i}}$ with the largest corresponding value of $\mathbf{\Delta\sigma_i}$ is selected as the optimal sensor and is assimilated using an ensemble Kalman Filter to update the climate metric $\mathbf{J}$.

First, the Kalman gain matrix $\mathbf{K}$ is computed from the covariance across the ensemble:

$$\mathbf{K} = \mathbf{cov}\left(\hat{\mathbf{Y}}_{\mathbf{i}}, \mathbf{J}_{\mathbf{i}}\right)\left[\mathbf{cov}\left(\hat{\mathbf{Y}}_{\mathbf{i}}\right) + \mathbf{R}\right]^{-1} \quad (2)$$

This is subsequently used to update $\mathbf{J}$, by accounting for the reduction in variance due to the assimilation of proxy $\hat{\mathbf{Y}}_{\mathbf{i}}$:

$$\mathbf{J}_{\mathbf{new}} = \mathbf{J} - \mathbf{K}\hat{\mathbf{Y}} \quad (3)$$

Proxy $\hat{\mathbf{Y}}_{\mathbf{i}}$ is then removed from the network of potential proxy sites, with $\mathbf{\Delta\sigma_i}$ set equal to 0. The process is then iteratively continued, returning to Eqn (1), until all potential proxy sites are ranked.

Hakim and others (2020) refer to the process described above as a 'blank slate' test. The blank slate experiment assumes no prior information, as it does not account for the influence of existing ice core records. In contrast, the augmented network experiment begins by applying the Kalman update equations (Eqns 2 and 3) to existing proxy sites to account for the variance constrained by existing ice core records; only after this is the optimal sensor algorithm (Eqns 1–3) applied.

2.3 Climate metric

The optimal sensor analysis is a scalar optimization problem; the scalar in question is the climate metric $\mathbf{J}$, which is distributed across an ensemble. We test four possible values of $\mathbf{J}$, evaluating two different climate variables and two different climate state ensembles.

The climate variables in question are two continental-scale metrics: 1) annual Antarctic accumulation, which can be used to

Downloaded from https://www.cambridge.org/core. 15 Nov 2026 at 21:07:29, subject to the Cambridge Core terms of use.

calculate sea level mitigation, and 2) annual Antarctic temperature, which provides insight into the temperature-accumulation relationship. Notably, our metrics for the 'representativeness' of an ice core site reflect variability on a continental, rather than a regional scale.

Separate experiments with each metric are performed for each of AIS, WAIS and EAIS. The metrics are calculated as either a spatial integration (for accumulation) or a spatial average (for temperature), across the region in question. The results can be interpreted as finding the locations that best constrain the variability in the climate metric across all of Antarctica, West Antarctica or East Antarctica, respectively. We highlight that we are targeting annual resolution to simulate high-resolution shallow ice cores spanning the past ~200 years.

We evaluate two different climate ensembles: a Multi-Model Ensemble ('MME') of nine different CMIP5 Last Millennium Simulations and a Multi-Reanalysis Ensemble ('MRE') of four different atmospheric reanalyses. The inclusion of multiple models with different spatial covariance structures minimizes structural uncertainty, and has been shown to increase climate reconstruction skill (Goosse and others, 2010; Steiger and others, 2014; Parsons and others, 2021).

The MME is constructed by randomly drawing 100 years from each of nine different CMIP5 Last Millennium Simulations (850–1850 CE), following Eswaran and others (2024). All models are regridded to the individual model (CCSM4) with the highest resolution (0.9375° × 1.25°, latitude-longitude), using bilinear interpolation. The nine models included are CCSM4 (Gent and others, 2011), iCESM (Brady and others, 2019), BCC-CSM1.1 (Wu and others, 2014), CSIRO Mk3L (Phipps and others, 2012), FGOALS-s2 (Bao and others, 2013), GISS-E2-R (Schmidt and others, 2014), HadCM3 (Collins and others, 2001), IPSL-CM5A-LR (Dufresne and others, 2013) and MPI-ESM (Gutjahr and others, 2019).

The MRE is constructed by drawing 40 years (1980–2019 CE) from each of four different atmospheric reanalyses, following a similar procedure to Wang and Xiao (2023). This period is chosen because reanalysis products are of limited reliability prior to the satellite era (i.e., before 1979; Bromwich and others, 2007; Schneider and Fogt, 2018; Bromwich and others, 2024). The four reanalyses included are ERA5 (Hersbach and others, 2020), MERRA-2 (Gelaro and others, 2017), CFSR (Saha and others, 2014) and JRA-55 (Kobayashi and others, 2015). Reanalyses are regridded to the MME resolution to allow for a consistent comparison.

The MRE and MME offer complementary strengths and weaknesses. The MME is a far larger ensemble and samples a broader range of plausible climate states; nevertheless, individual ensemble members of the MRE are theoretically a better representation of the 'true' climate state, as they are constrained by instrumental observations. The CMIP5 simulations that make up the MME have been shown to consistently overestimate Antarctic precipitation (Palerme and others, 2017); furthermore, their coarse resolution renders them unable to fully capture the orographic spatial variability of temperature and precipitation (Tang and others, 2018). The reanalyses that make up the MRE are a generally more skillful representation of precipitation and temperature spatial covariance than the MME models (Tang and others, 2018); they have been found to present spurious climatic trends (Bromwich and others, 2011), but with a notable improvement since 1979 (Bromwich and others, 2024). The structural uncertainty is relatively high in the MRE, with differing levels of agreement with observations (Boisvert and others, 2018); the highest spread and bias occur in the low-accumulation interior of East Antarctica (Palerme and others, 2017).

2.4 Proxy estimates

The optimal sensor algorithm requires estimates of potential ice core proxy records (or 'proxy estimates'): $\hat{\mathbf{Y}}$. We test four possible values of $\hat{\mathbf{Y}}$, evaluating two different climate variables and two different climate state ensembles.

The climate state ensembles are the same as those used to construct **J**: namely, the MME and the MRE. In both cases, we evaluate 5794 potential proxy sites in total, corresponding to the gridscale resolution of CCSM4. By evaluating each Antarctic grid cell, we can assess how well individual ice core sites can constrain the variance in **J.**

The proxy estimates ($\hat{\mathbf{Y}}$) simulate either ice core accumulation or water isotope records, but are drawn from the climate state ensemble rather than from the actual proxy records. If **J** is a time series of annual Antarctic accumulation, proxy estimates simulate accumulation by drawing from the annual precipitation for each grid cell from the climate state ensemble. Because the variability between accumulation and precipitation in Antarctica is highly correlated and precipitation is the dominant term in Antarctic surface mass balance (Bromwich, 1988; Lenaerts and others, 2019), we treat the two as equivalent. If **J** is instead temperature, proxy estimates simulate $\delta^{18}O$ by drawing from the average annual surface air temperature for each grid cell. This approach assumes that temperature can be related to $\delta^{18}O$, as commonly done in proxy system models (e.g. Dee and others, 2016). While this simplification enables practical assessment of each site's potential to constrain **J**, it also requires the interpretation of results within the context of these assumptions.

Our method does not account for spatial uncertainty in the $\delta^{18}O$-temperature relationship. Analyses of isotope-enabled climate models and ice cores indicate significant regional differences in this relationship, with the relationship being weaker in East Antarctica (Goursaud Oger and others, 2024). Although nonlinear proxy system models (PSMs) can be used to estimate spatial variability in isotope fractionation (e.g. Markle and Steig, 2022), the nonlinear PSMs also have uncertainties that can erode reconstruction skill (Dee and others, 2016; Steiger and others, 2017). Paleoclimate data assimilation studies show that nonlinear PSMs may not yield improvements when compared to simpler linear calibrations, especially for ice core $\delta^{18}O$ (Dee and others, 2016), except in cases where an isotope-enabled model is used (Steiger and others, 2017).

Given these challenges, we do not employ nonlinear PSMs to model spatial variability and uncertainty of the $\delta^{18}O$–temperature relationship; instead, we derive $\delta^{18}O$ proxy estimates from surface air temperature, assuming that the uncertainty is spatially uniform. While evaluating the influence of spatial variability in our ability to relate $\delta^{18}O$ data and temperature on optimal ice core site selection is beyond the scope of this study, it represents an important direction for future investigation. Another avenue for further work is to explore the calibration of accumulation records to temperature, or the inclusion of an isotope-enabled model as a source of proxy estimates (e.g. Dalaiden and others, 2020). We emphasize that our study assumes linearity between temperature and $\delta^{18}O$, and our temperature results should be taken with this assumption in mind.

Downloaded from https://www.cambridge.org/core. 15 Nov 2026 at 21:07:29, subject to the Cambridge Core terms of use.

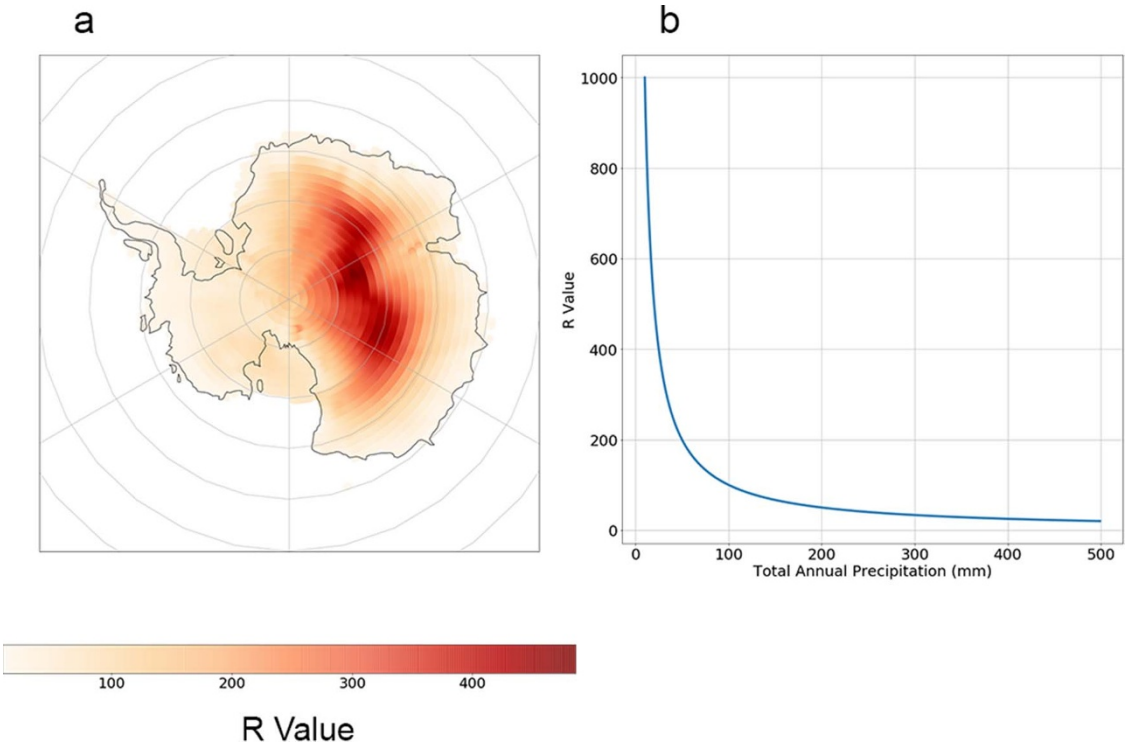


Figure 2. Accumulation-based *R* values, calculated using Eqn (4). *R* values are shown in (a). across the Antarctic Ice Sheet for all potential ice-core sites, with the accumulation estimates sourced from ERA5 reanalysis, and in (b) as a function of accumulation rate.

2.5 Proxy uncertainties

Numerous sources of uncertainty impede the ability to extract a meaningful and accurate signal from an ice core. We express the uncertainty with the error matrix **R**. We scale the uncertainty to the inverse accumulation rate, as the accumulation rate affects both the timescale accuracy and spatial representativeness, elaborated upon below. The diagonal elements (hereafter referred to as the '*R* values') vary with the inverse of accumulation rate:

$$\mathbf{R} = \boldsymbol{\alpha}\mathbf{P}^{-1} \tag{4}$$

Here, **P** is an $n \times n$ diagonal matrix, with the nth diagonal representing the average (1981–2020) total annual precipitation at the nth evaluated ice core site, drawn from ERA5 reanalysis. The scaling constant $\boldsymbol{\alpha} = 10^4$ is empirically derived from data assimilation methods using the error variance in linear calibration to estimate *R* values (e.g. Hakim and others, 2016; Tardif and others, 2019; Eswaran and others, 2024).

We now elaborate on our discussion of proxy (ice core) uncertainty. We consider two primary sources of ice core uncertainty: timescale uncertainty and spatial representation uncertainty. We again note that this study targets high-resolution (i.e. annually resolved) ice cores, which renders the impact of diffusion insignificant in all but very low-accumulation records (Cuffey and Steig, 1998).

Annually resolved ice core records are dated through identification of seasonal variations in trace chemistry impurities and stable water isotope concentrations. When the absolute accumulation rate is low (e.g. on the East Antarctic Plateau), the accurate identification of annual layers becomes increasingly challenging (e.g. Alley and others, 1997). This indicates that ice core uncertainty is dependent on accumulation rate, with low-accumulation sites having high uncertainty and vice versa (Casado and others, 2020; Servettaz and others, 2020). Nevertheless, accumulation rate is not the only factor in annual layer identification. For instance, high marine sulfate deposition at coastal sites can obscure the seasonal cycle and volcanic markers (Dixon and others, 2005; Steig and others, 2005; Winstrup and others, 2019; Hoffmann and others, 2022). Another exception is surface melt at high-temperature sites (e.g. the Antarctic Peninsula), which can bias the seasonal cycle and smooth the $\delta^{18}O$ record (e.g. Orsi and others, 2015; Hoffmann-Abdi and others, 2023). These site-specific features must be evaluated, yet the general trend of uncertainty decreasing with accumulation is empirically supported (Fig. S2). Thus, we choose that **R** values vary inversely with accumulation rate (Eqn 4); using our method, low-accumulation proxy sites (e.g. on the East Antarctic Plateau) are penalized, while high-accumulation sites (e.g. in coastal West Antarctica) are rewarded (Fig. 2a). Generally speaking, our method serves to filter out extremely low-accumulation sites (Fig. 2b).

Another source of uncertainty in ice core records is that of spatial representation: is the ice core truly representative of the area for which it is supposed to provide a climate history (e.g. the relevant grid cell in the model or reanalysis)? As ice core length scales are on the order of centimeters while grid cells are on the order of kilometers, no ice core site can be fully representative of its grid cell. We identify three considerations in this question of spatial uncertainty: the ice velocity, orography and wind.

Except at ice divides, ice with increasing depth has been deposited at increasing distance upstream from the drilling site due to ice flow. We create a simple heuristic to assess the spatial representativeness of an ice core due to ice flow by comparing the size of our grid cells with the ice displacement for a representative reconstruction timescale. As we target annually resolved reconstructions from high-resolution records, we set the representative

Downloaded from https://www.cambridge.org/core. 15 Nov 2026 at 21:07:29, subject to the Cambridge Core terms of use.

timescale to 200 years (i.e. for a reconstruction from 1800 to 2000 CE). Given a CMIP grid resolution of approximately 60 km and a 200-year reconstruction period, we find that an upper bound on the spatial representativeness of ice core records will be when ice velocity exceeds 300 m a^{-1}. This threshold is only exceeded within ice shelves and terminal portions of ice streams (Rignot and others, 2022); while sections of fast-moving ice certainly exist elsewhere on the continent behind the grounding line, nearby slow-moving regions (e.g. ice domes and ice rises) can still be found and are much better drilling locations. Therefore, we do not consider ice shelves when assessing potential ice core sites, but we do consider ice rises which are surrounded by ice shelves. We note that the 300 m a^{-1} value is in practice a significant overestimate; the vast majority of existing ice cores have been drilled at sites with a velocity of over an order of magnitude lower. Furthermore, significant climatic variability can occur within a single grid cell due to the local orography.

While orography and wind certainly influence the spatial representation uncertainty, we do not find that it can be quantified in a non-arbitrary fashion; therefore, we do not incorporate a quantitative measure of orography into **R**. Generally, climatological variability within a grid cell will vary with orographic variability, due to elevation-dependent changes (e.g. the atmospheric lapse rate) and wind-based snow redistribution; thus, as orographic complexity increases, individual ice core sites are less likely to be spatially representative of the surrounding area (Cavitte and others, 2023). Furthermore, it is more logistically difficult to drill in mountainous and other topographically complex regions (e.g. coastal regions and ice rises within or bounding ice shelves). A comparison of ice core accumulation records at ice rises to ice-penetrating radar data reveals that the spatial representativeness of ice cores tends to vary with orographic complexity and orography-wind interactions (Cavitte and others, 2023; Wauthy and Dalaiden, 2026). However, these factors are challenging to quantify and ice cores have still been drilled at mountainous locations in Antarctica (e.g. Stenni and others, 1999; Goodwin and others, 2016) and coastal ice rises (e.g. Philippe and others, 2016; Winstrup and others, 2019; Neff, 2020; Hoffmann and others, 2022), which show good agreement with ERA5 (Fig. S2a and b). Nevertheless, we qualitatively consider these factors when we present our drilling case studies below.

2.6 Existing ice core records

In order to conduct the 'augmented network' and 'redrilling' experiments, we first account for the influence of the existing ice core proxy network. We note that the proxy records themselves are not assimilated; instead, we assimilate synthetic 'proxy estimates' ($\hat{\mathbf{Y}}$) derived from climate models or reanalyses at each existing ice core location. To represent a given water isotope or accumulation record, we create a synthetic record from the precipitation or surface air temperature time series for the relevant grid cell; this is distributed across the ensemble. This allows us to analyze the relationship between a given site in the ensemble and the climate metric calculated from the same ensemble.

We assimilate proxy estimates ($\hat{\mathbf{Y}}$) from 56 sites with accumulation records and 54 sites with water isotope records in total (Fig. 1a). These sites include 54 accumulation sites (Thomas and others, 2017) and 49 water isotope sites (Stenni and others, 2017) from the PAGES 2k databases. We additionally include estimates of accumulation from the B40 site (Medley and others, 2018), accumulation and $\delta^{18}O$ from the South Pole ice core (Kahle and others, 2021), and $\delta^{18}O$ from Derwael Ice Rise (Philippe and others, 2016), PIG2010, DIV2010 and THW2010 (Criscitiello and others, 2013; Medley and others, 2013).

3. Results

3.1 Blank slate tests

We run the standard optimal sensor algorithm, assuming no prior influence (i.e. no existing ice cores) and with all grid cells within the grounding line (Zwally and others, 2012) as potential proxy sites. Figure 3 shows the resulting calculated optimal network of 10 ice cores, and the percentage of variance in the climate metric that is theoretically constrained by each potential ice core site. We note that comparing the values of constrained variance between independent experiments can be misleading. The choice of 10 cores approximates how many ice cores could be expected to be drilled over a period of several years.

The results indicate that the variance in annual Antarctic accumulation can be best constrained by sites around the WAIS Divide and the southern Ross Ice Shelf (Fig. 3a and b), likely due to high covariance in this region with Antarctic accumulation (Figs S1a and b). Consequently, the calculated accumulation optimal networks are extremely clustered. Results from both the MME and MRE calculations strongly favor sites in the Transantarctic Mountains at the southern edge of the Ross Ice Shelf, selecting four and three sites in this region, respectively. Records from these regions show high potential to constrain variability in both WAIS-specific and EAIS-specific accumulation (Fig. S3). Agreement between the MME and MRE is a sign of confidence in the results because they have complementary strengths and weaknesses: the larger size of the MME accounts for a broader range of plausible climate states, but the covariance structures of the MRE are supported by instrumental observations.

Additionally, for the AIS accumulation experiments, the MME selects two sites near the existing South Pole Ice Core (Kahle and others, 2021; Fig. 1a), while the MRE selects three sites slightly north of the proposed Hercules Dome Ice Core (Fudge and others, 2023; Fig. 1b). The optimal sensor algorithm selects 'clusters' of multiple sites when these locations have strong covariance with the continental climate metric. As all ice core records have inherent variability and noise, a stronger signal can be extracted from the noise with multiple adjacent records (Comboul and others, 2015).

Sites at the southern edge of the Ross Ice Shelf show high potential in both the MME and MRE to constrain annual Antarctic temperature (Fig. 3c and d, Fig. S4). The MME additionally selects a cluster of sites near the Brunt Ice Shelf in DML, a region which has a particularly high potential to constrain temperature variability in EAIS specifically (Fig. S4). The MRE network is much more dispersed, but both the MRE and MME select sites in the Transantarctic Mountains and near Troll Station in DML. Coastal sites along the Amundsen and Bellingshausen Sea (e.g. Neff, 2020; Thomas and others, 2024) show high potential in both the MME and MRE to constrain WAIS-averaged temperature variability (Fig. S4).

3.2 Augmented network tests

While the blank slate tests provide insight into which regions of Antarctica best constrain the variance in annual Antarctic temperature and accumulation, a network of records already exists (Fig. 1a). We again run the optimal sensor algorithm with all grid cells treated as potential proxy sites, but now we first account for

Downloaded from https://www.cambridge.org/core. 15 Nov 2026 at 21:07:29, subject to the Cambridge Core terms of use.

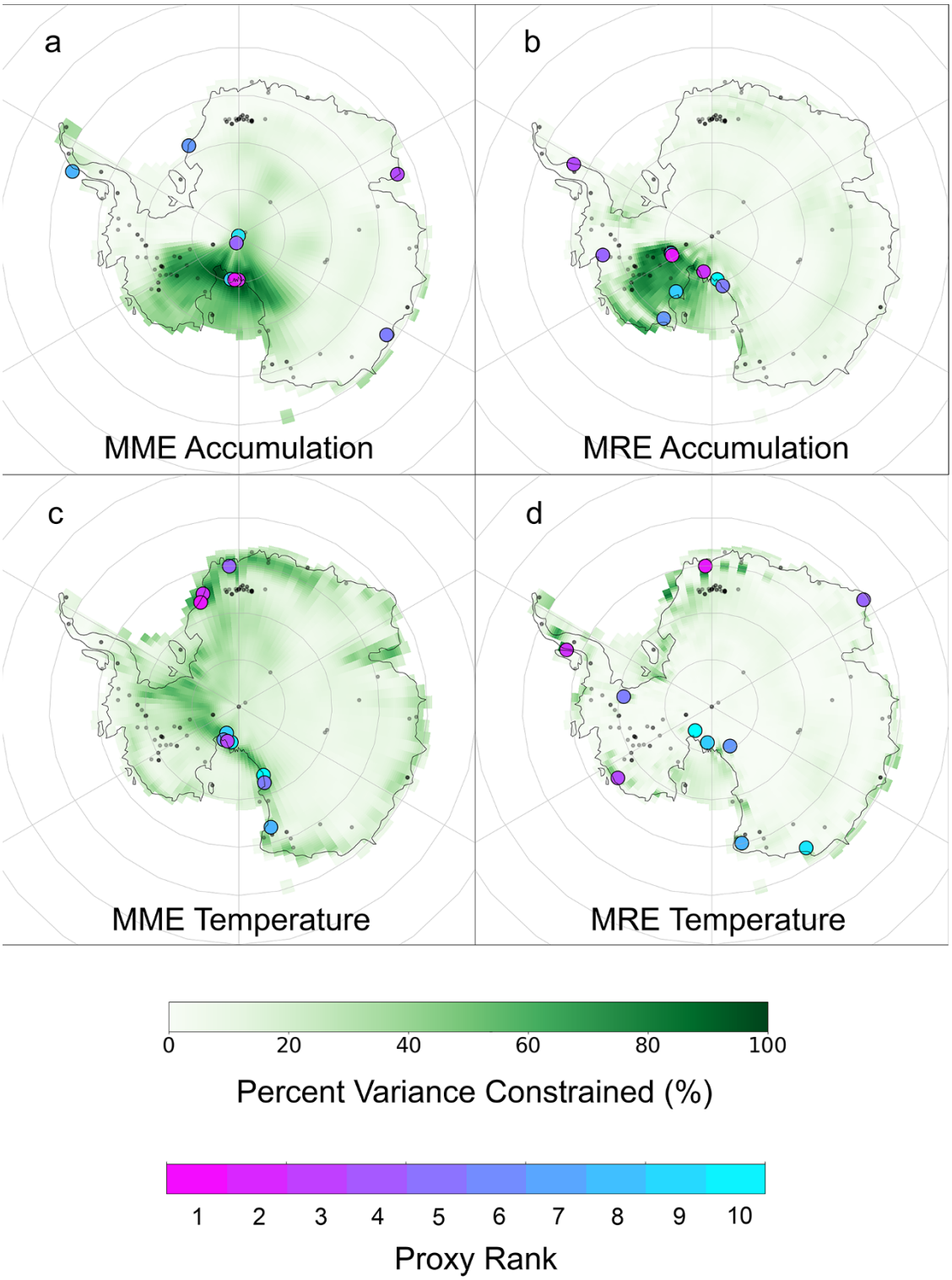


Figure 3. 'Blank slate' optimal Antarctic ice-core accumulation (a, b) and $\delta^{18}O$ (c, d) networks for reconstructing annual Antarctic accumulation (a, b) and temperature (c, d), respectively. Climate estimates are sourced from the MME (a, c) and MRE (b, d). The optimal 10-site network is shown, with green shading indicating the normalized variance in the climate metric that is constrained across the ensemble by an ice-core record from each possible site. Gray dots indicate existing ice-core locations.

the variance constrained by the 110 existing ice core records of accumulation or $\delta^{18}O$.

The influence of the existing proxy network is readily apparent with the accumulation experiments. In the blank slate tests, sites across much of WAIS have high potential to constrain the variance in annual Antarctic accumulation (Fig. 3a and b, Fig. S3). Once the influence of existing records is accounted for, this potential dramatically drops (Fig. 4a and b, Fig. S3). This is a positive sign, implying that current ice cores in WAIS are well-placed to constrain the variance in annual Antarctic accumulation. For new accumulation

Downloaded from https://www.cambridge.org/core. 15 Nov 2026 at 21:07:29, subject to the Cambridge Core terms of use.

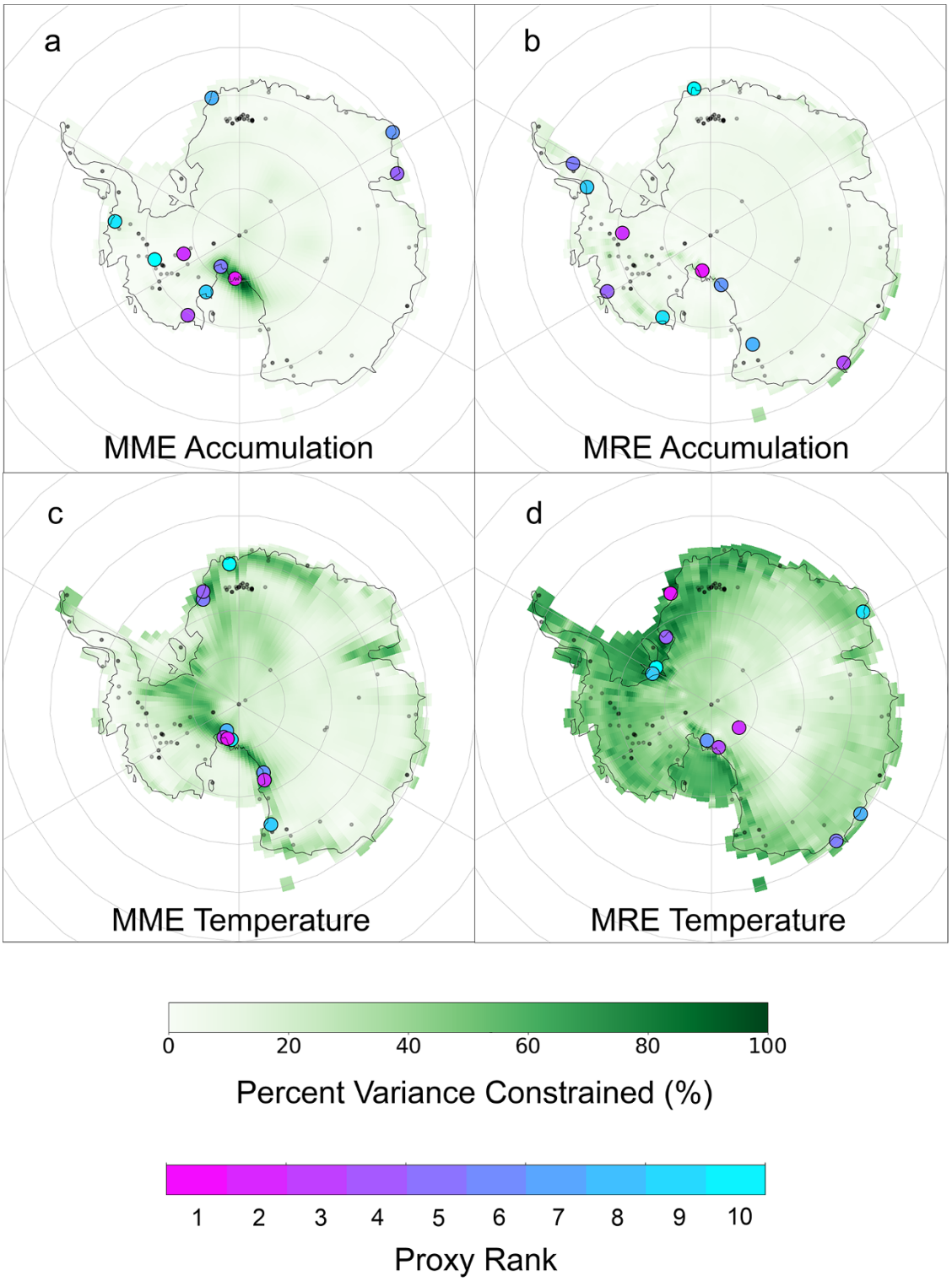


Figure 4. 'Augmented network' optimal Antarctic ice core accumulation (a, b) and $\delta^{18}O$ (c, d) networks for reconstructing Antarctic accumulation (a, b) and temperature (c, d), respectively. Climate estimates are sourced from the MME (a, c) and MRE (b, d). The optimal 10-site network is shown, with green shading indicating the normalized variance in the climate metric that is constrained across the ensemble by an ice-core record from each possible site. Gray dots indicate existing ice-core locations.

sites, the MME strongly favors a small region at the southern end of the Ross Ice Shelf, in the Transantarctic Mountains. The MRE additionally finds that sites around the Brunt Ice Shelf in western DML have high potential to constrain variance in annual EAIS accumulation (Fig. S5).

For the temperature experiments, results from both the MME and MRE calculations select a cluster of sites at the southern end of the Ross Ice Shelf. The MME selects a second cluster further north in the Transantarctic Mountains, in the vicinity of McMurdo Station. It selects a third cluster on the edge of the Brunt Ice

Downloaded from https://www.cambridge.org/core. 15 Nov 2026 at 21:07:29, subject to the Cambridge Core terms of use.

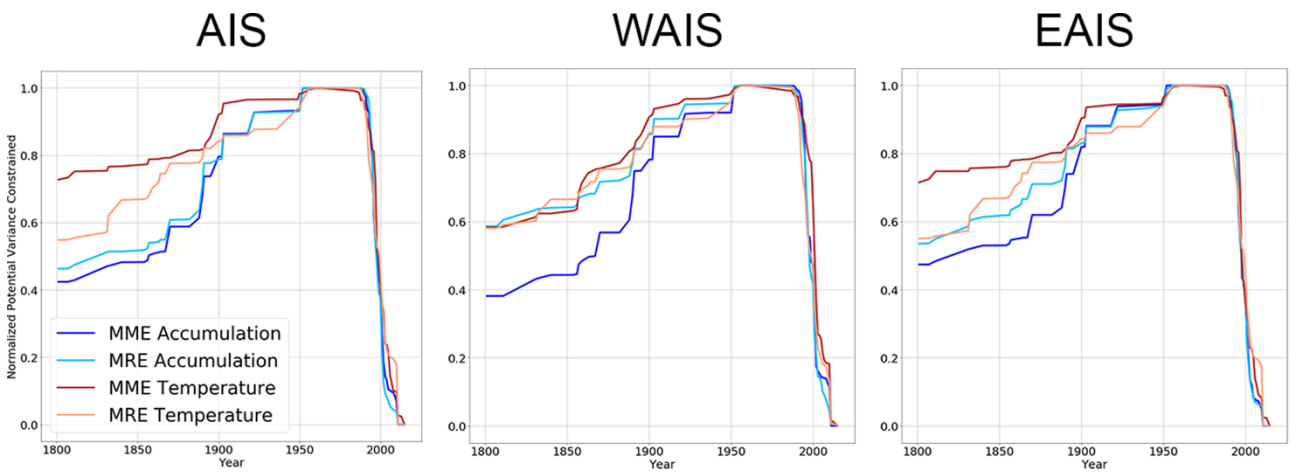


Figure 5. Percentage of the maximum possible normalized variance constrained by the existing Antarctic ice-core proxy network from 1800 to 2010 CE, evaluated for two climate variables (accumulation and temperature), two climate state ensembles (MME and MRE), and three regions: AIS, WAIS and EAIS. The maximum variance is constrained from 1962 to 1983; during this period, the chronologies of all evaluated ice core records overlap.

Shelf near Halley Research Station, which is particularly effective in constraining annual EAIS temperature (Fig. S6). Meanwhile, an MRE cluster is selected on ice rises in the Ronne Ice Shelf, near the existing Berkner Island ice core (Mulvaney and others, 2002; Fig. 1a), which also has good potential to constrain annual EAIS temperature. According to the MRE calculations, annual WAIS temperature can be well constrained by a cluster of sites near the Ellsworth mountains (Fig. S6). Finally, for all experiments except the MME temperature test, various miscellaneous sites are selected at coastal locations in East Antarctica, particularly near the existing Mawson and Dumont d'Urville stations (Fig. 1c); these primarily provide insight into annual EAIS temperature (Fig. S6).

3.3 Redrilling tests

The augmented network tests provide insight into where to drill a new ice core. However, they are predicated on the assumption that a continuous chronology exists for the entire existing ice core network throughout the period of interest. In reality, most existing cores were drilled more than two decades ago through efforts such as the International Trans-Antarctic Scientific Expedition (ITASE; Mayewski and others, 2005; Steig and others, 2005; Fig. 1b) and the European Project for Ice Coring in Antarctica (Stauffer and others, 2004). Indeed, of the 110 ice core records we evaluate, only 48 have a chronology that extends past 2000 CE and only 14 extend past 2010 CE; this is why many Antarctic climate reconstructions choose to terminate in 2000 (e.g. Medley and Thomas, 2019; Dalaiden and others, 2021). Additionally, these chronologies begin at different times; the 110 records we evaluate only have a complete overlap between 1962 and 1983 CE, which is mostly prior to the satellite era.

Thus, the effective variance constrained by the existing proxy network is a function of time, as some years will contain more information than others. We evaluate the variance constrained by the ice core network that exists for each individual year from 1800 to 2010 CE. Both climate ensembles and variables show a consistent pattern: starting from 1800 CE, our ability to reconstruct Antarctic climate steadily increases until the mid-to-late 20th-century, and then rapidly plummets starting in the mid-1990s (Fig. 5). These results indicate that our ability to reconstruct 21st-century Antarctic climate, using ice cores, is less than 10% that of the mid-20th century. This motivates the choice of our study, and others (e.g. Medley and Thomas, 2019), to terminate the period of reconstructive interest in 2000 CE. Thus, new ice core records for the 21st-century are strongly desired, in order to extend the presently limited overlap period with satellite-era reanalysis and contextualize modern changes.

Selecting and drilling at novel ice core sites is one method of gaining information about recent Antarctic climate variability, but another option is to redrill at existing ice core locations, thereby making their chronologies up to date. Our 'redrilling' tests address this latter question: which existing ice cores would be best to redrill and bring up to date? Fig. 6 shows the potential variance in annual Antarctic accumulation and temperature constrained by accumulation and $\delta^{18}O$ proxy estimates from all existing ice core sites.

The accumulation tests (Fig. 6a and b) contain a significant regional disparity. Results from both the MME and MRE experiments indicate that WAIS sites are by far the most optimal to redrill. This is likely because this region has the highest local covariance with continental-scale precipitation (Fig. S1). We note that many of the ITASE sites in WAIS (Fig. 1a) are chosen by both ensembles as being highly optimal to redrill. From now on, we use 'ITASE' as a shorthand for the West Antarctic records obtained through the U.S. component of the International Transantarctic Scientific Expedition.

By contrast, the $\delta^{18}O$ tests (Fig. 6c and d) offer a less immediately obvious conclusion, with the MME and MRE experiments showing divergent results across a variety of regions. The MRE results suggest that redrilling one of the numerous ice cores in interior DML (Oerter and others, 1999), as done by Winton and others (2024), would be advantageous. Other sites include the Mount Erebus Saddle core (Rhodes and others, 2012) and the Bruce Plateau core (Goodwin and others, 2016) on the Antarctic Peninsula. The MME instead favors sites in coastal, rather than interior, DML, such as IND-22/B4 (Thamban and others, 2011); it is also more favorable to sites in WAIS than the MRE. This divergence can likely be attributed to the fact that the spatial temperature covariance patterns between the MME and MRE are quite dissimilar (Fig. S1c and d), indicating the challenges in accurately constraining temperature over the AIS.

Downloaded from https://www.cambridge.org/core. 15 Nov 2026 at 21:07:29, subject to the Cambridge Core terms of use.

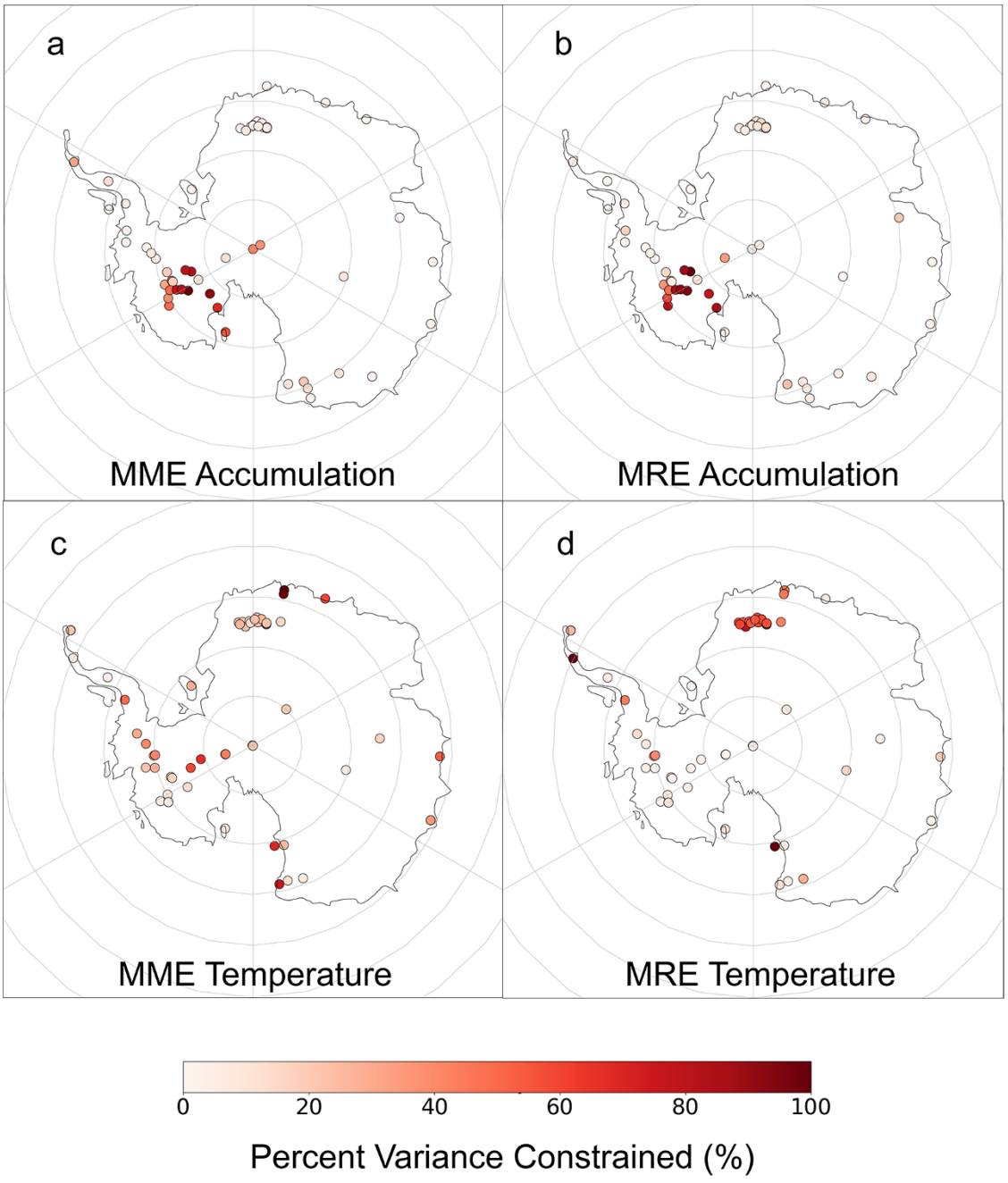


Figure 6. Normalized percent of variance in annual Antarctic accumulation (a, b) and annual Antarctic temperature (c, d) constrained by accumulation (a, b) and $\delta^{18}O$ (c, d) at existing ice-core sites. Proxy estimates ($\hat{\mathbf{Y}}$) are sourced from the MME (a, c) and MRE (b, d).

4. Discussion

Our results identify potential locations for new ice core drilling that are best for the purposes of reconstructing changes in Antarctic-wide annual temperature and accumulation. The results do not evaluate site-specific limitations such as ice velocity and topography, or local influences on accumulation such as precipitation intermittency, seasonality and wind redistribution. We describe the following three case studies to illustrate the importance of additional site-specific understanding, and do not explicitly propose them as future ice coring sites. Instead, our goal is to illustrate that despite the relatively large spatial scale of our analysis, there are potential drilling sites that could be targets. In all cases, proposals to drill specific locations will benefit from in situ data collected at the site, including, but not limited to, conducting ice-penetrating radar surveys to understand the glaciological setting and drilling short firn cores covering the satellite era to establish the representativeness of preserved climate records. We conclude the discussion by addressing limitations of the current data and methodology and suggesting avenues for future work.

4.1 Case studies

Here, we present three case studies of potential new shallow ice coring projects: 1) drilling a new core at Crary Ice Rise (CIR); 2) drilling a new core at Lyddan Ice Rise; and 3) redrilling the US-ITASE cores collected in the early 2000s in WAIS

Downloaded from https://www.cambridge.org/core. 15 Nov 2026 at 21:07:29, subject to the Cambridge Core terms of use.

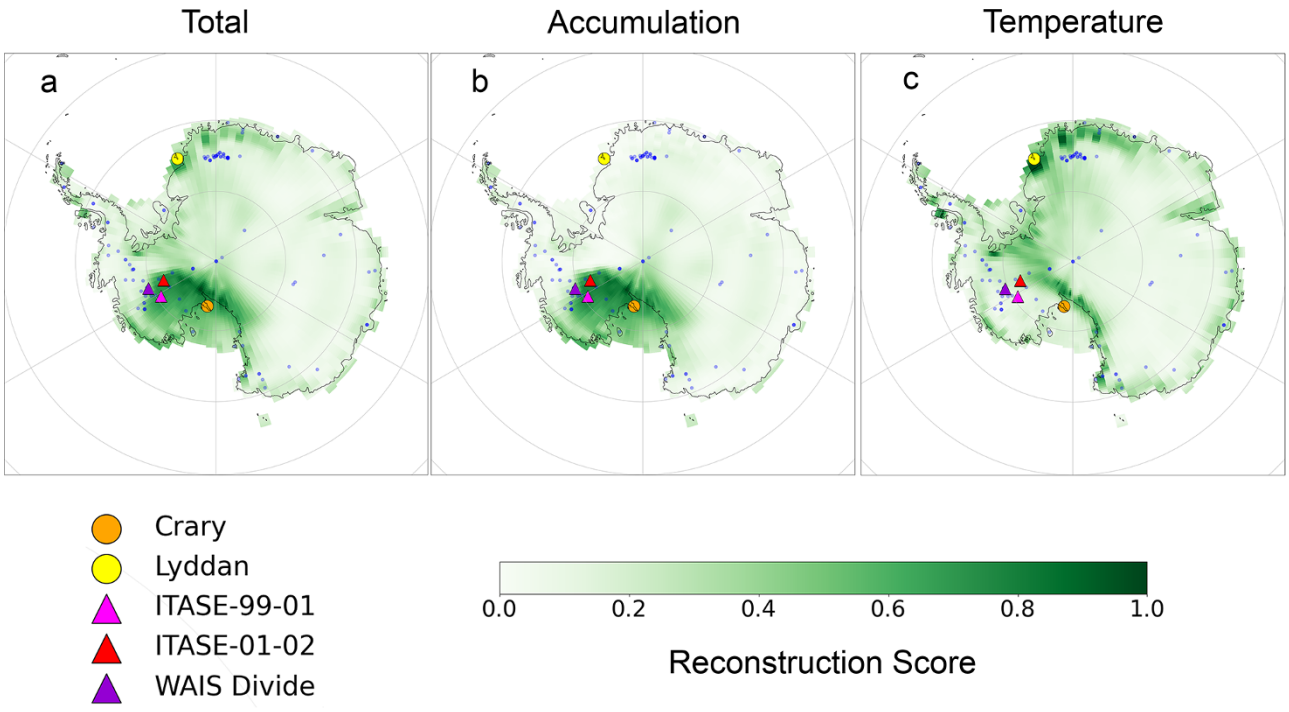


Figure 7. 'Optimality scores' for each potential Antarctic ice-core site, calculated by taking the root mean square of the normalized percent constrained variance for each grid cell across (a) all four 'blank slate' experiments ('Total'), (b) the two accumulation experiments, and (c) the two temperature experiments (Figure 3). The sites of three drilling case studies: Crary Ice Rise, Lyddan Ice Rise and ITASE core redrilling at ITASE-99-01, ITASE-01-02 and WAIS Divide are displayed.

Table 1. Physical characteristics of five potential ice-core sites: Crary Ice Rise, Lyddan Ice Rise, ITASE-99-01, ITASE-01-02 and WAIS Divide. We include topographic information from Bedmachine (Morlighem and others, 2020), ice velocity (MacAyeal and others, 1987; Kaspari and others, 2004; King and others, 2004; Koutnik and others, 2016) and accumulation rate from surface observations (Bindschadler and others, 1990; Kaspari and others, 2004; King and others, 2004; Orsi and others, 2012).

Ice-core site	Latitude	Longitude	Region	Surface elevation (m above sea level)	Bed elevation (m above sea level)	Ice thickness (m)	Ice velocity (m a^{-1})	Accumulation rate (m a^{-1} ice equivalent)
Crary Ice Rise	−83.05°	−172.50°	Ross Ice Shelf	130	−400	530	Negligible	0.11
Lyddan Ice Rise	−74.05°	−21.00°	Brunt and Riiser-Larsen Ice Shelves	260	10	240	Negligible	0.30
ITASE-99-01	−80.62°	−122.63°	West Antarctic Ice Sheet	1300	−1110	2410	20	0.15
ITASE-01-02	−82.00°	−110.01°	West Antarctic Ice Sheet	1760	−180	1940	10	0.19
WAIS Divide	−79.46°	−112.09°	West Antarctic Ice Sheet	1780	−1680	3460	3	0.22

(Table 1). These case studies were chosen to combine both climatic reconstructive ability (Fig. 7) and logistical feasibility. We emphasize that our study identifies ice core sites to constrain our two chosen climate metrics: annual accumulation and annual temperature. As noted above, our methodology does not quantify all the relevant complexities of ice core site selection, and our case studies should not be taken as a formal proposal to drill at these locations. Nevertheless, these case studies represent promising targets for future drilling and illustrate how our data-driven optimization approach can be adapted to account for real-world site selection and logistical constraints.

4.2 Crary Ice Rise

Locations at the southern edge of the Ross Ice Shelf and within the Transantarctic Range are consistently identified as good drilling sites (Figs 3a–d, 4a–d, Figs S3–4). Climate records from this region can constrain both annual Antarctic accumulation and temperature when averaged across each of AIS, WAIS and EAIS, yet no ice cores have been drilled in this region to date (Figure 1a and 8a), excepting a single 8-year firn core (Markle and others, 2012). The Ross Ice Shelf and Transantarctic Range regions both present challenges for obtaining ice core records. The Ross Ice Shelf and associated ice streams have velocities of over 100 m a^{-1} (Fig. 8b), compared to velocities of under 10 m a^{-1} at most existing ice core sites on the AIS (Rignot and others, 2022); ice core sites on ice shelves thus may not accurately reflect the site history. Drilling in the Transantarctic Mountains generates logistical difficulties as well as raising questions about spatial representativeness, where high orographic variability (Figure 8c) combined with wind-borne snow transport leads to high climatic variance within a small geographic area (King and others, 2004; Cavitte and others, 2023).

Downloaded from https://www.cambridge.org/core. 15 Nov 2026 at 21:07:29, subject to the Cambridge Core terms of use.

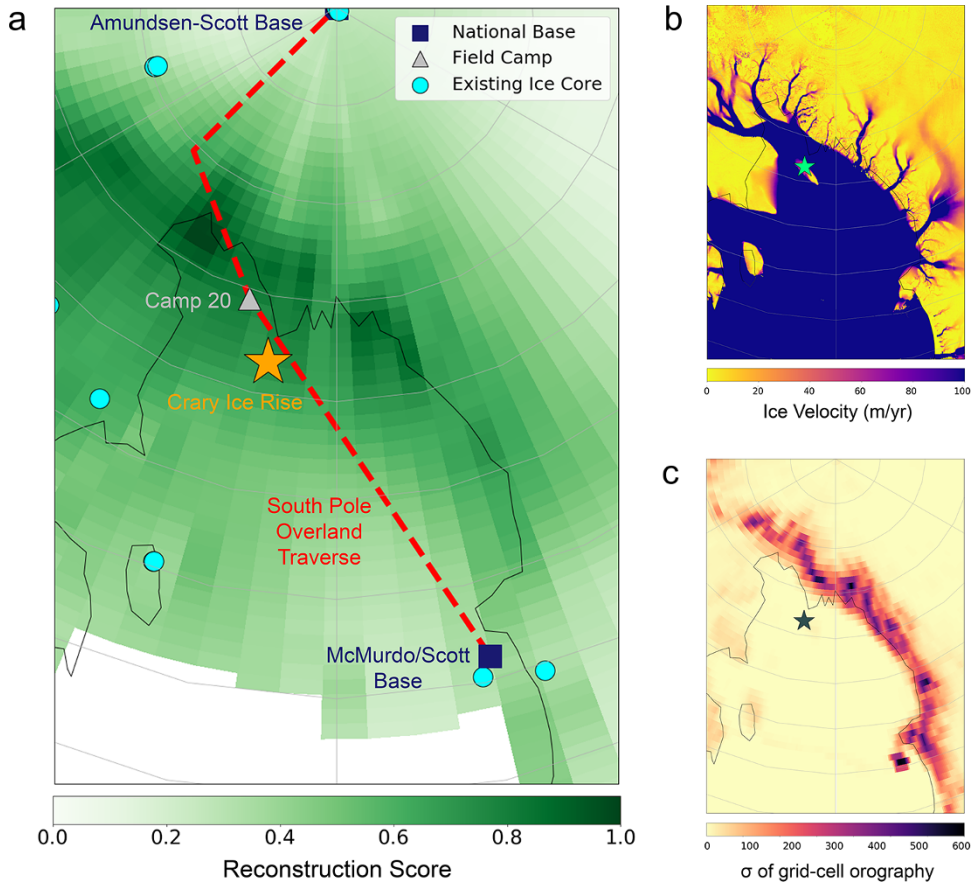


Figure 8. (a) 'Optimality scores' (an inset of Figure 7a); (b) ice velocity (Rignot and others, 2022); and (c) standard deviation of ERA5 grid-cell orography (Hersbach and others, 2020), shown for the Ross Ice Shelf region. Crary Ice Rise is indicated with a star; also displayed are existing ice cores, national bases and field camps and the South Pole Overland Traverse route between McMurdo and Amundsen-Scott stations.

Altogether, this begs the question: is there a viable path between the Scylla of rapid ice flow and the Charybdis of mountainous topography?

CIR is a small ice rise close to the southern edge of the Ross Ice Shelf, which formed ~1100 years ago when the Ice Shelf re-grounded on marine sediment (Catania and others, 2012). At a pinning point of the Ice Shelf, ice flow at CIR reduces to near-zero and the accumulation rate is about 0.11 m a^{-1} ice equivalent (Table 1). Ice rises provide a solution to the problem of drilling on ice shelves, as they show far lower rates of ice flow (e.g. Matsuoka and others, 2015); this is why numerous ice cores have been drilled on Antarctic ice rises, such as Derwael Ice Rise (Philippe and others, 2016), Siple Dome (Taylor and others, 2004), Roosevelt Island (Winstrup and others, 2019), Skytrain Ice Rise (Hoffmann and others, 2022) and the Amundsen Sea Coast (Neff, 2020). We note that there are challenges associated with drilling on coastal ice rises, but these can be mitigated. High marine sulfate deposition can impede accurate dating, but alternate dating mechanisms such as methane matching can be utilized (Winstrup and others, 2019) and CIR is far from the coast. Ice rises show high local accumulation variability due to blowing snow and wind-orography interactions (King and others, 2004; Cavitte and others, 2023), indicating that care should be taken to choose a site that is spatially representative of the surrounding area. Any drilling proposal at CIR should additionally account for the impact of extreme precipitation events (Turner and others, 2019). The drilling and analysis of a shallow core (~20 years) would provide an effective way to assess the spatial representativeness of the ice core site.

No ice core has been drilled yet at CIR; however, it has been an active site for glaciological fieldwork, including a recent study of the evolution of the ice rise using radar transects (Hillebrand and others, 2021). This existing ice-penetrating radar data will significantly aid site selection efforts. Hillebrand and others (2021) find discontinuous layers at 250–300 m above the bed, which are composed of former Ross Ice Shelf marine ice. However, the uppermost ~200 m contains well-preserved and spatially continuous internal layering from local meteoric accumulation that is more than thick enough to cover the past 200 years and likely considerably more. Coring to recover both this meteoric snow accumulation as well as access former Ross Ice Shelf marine ice would yield valuable insight not only into Ross Sea regional climate but also the former sub-ice shelf marine environment.

CIR is additionally an active site of interest for recent mass change, motivated by the effects of ice stream deceleration on the embayment buttressing regime of the Ross Ice Shelf (Verboncoeur and others, 2025). Previous work at CIR shows that logistical support is feasible; it is located just off the South Pole Overland Traverse (SPOT) between McMurdo and Amundsen-Scott stations and close to the existing Camp 20 field camp (Fig. 8a). As part of the SWAIS 2C project (Patterson and others, 2022), an international team will drill a sediment core at CIR, with logistical support being provided by SPOT.

Downloaded from https://www.cambridge.org/core. 15 Nov 2026 at 21:07:29, subject to the Cambridge Core terms of use.

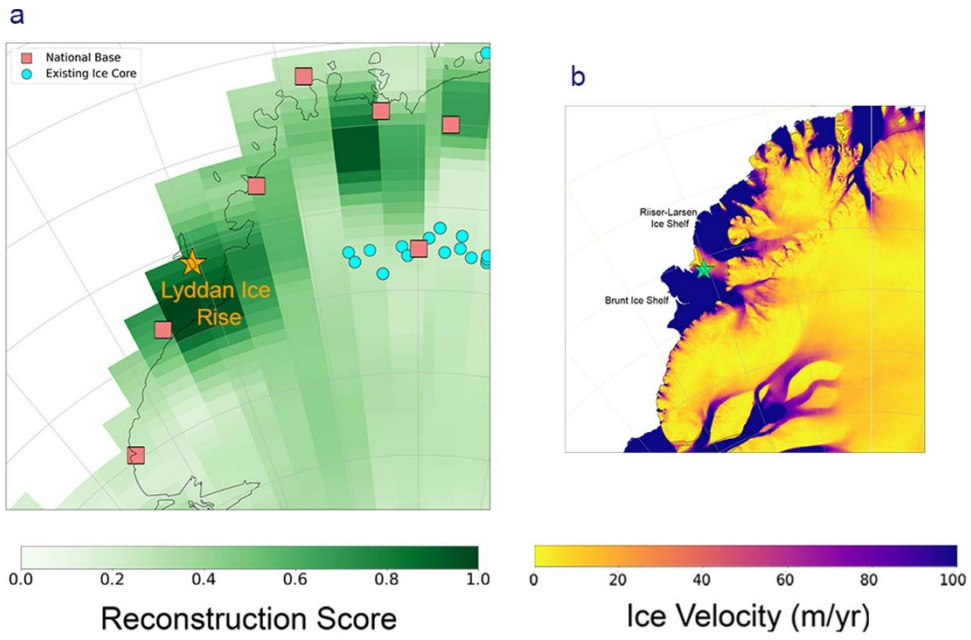


Figure 9. (a) Temperature 'optimality scores' (an inset of Figure 7c), and (b) ice velocity (Rignot and others, 2022) shown for the western Dronning Maud Land region. Lyddan Ice Rise is indicated with a star; existing ice cores and national bases are also displayed.

4.3 Lyddan Ice Rise

Our analysis suggests that the best location for reconstructing annual Antarctic temperature, particularly in EAIS, is coastal western DML in the vicinity of the Brunt and Riiser-Larsen ice shelves (Figure 7c and 9, Fig. S4). Our results also indicate that coastal western DML is a good location to complement existing ice cores to improve reconstructions of 19th–20th century annual EAIS accumulation (Figure S5) by drilling at high accumulation coastal sites in EAIS (e.g. Jackson and others, 2023; Vance and others, 2024).

Numerous ice cores have been drilled in the interior DML (e.g. Oerter and others, 1999; Medley and others, 2018; Winton and others, 2024) yet are primarily outside the coastal regions we identify as highly correlated with annual Antarctic-wide temperature. The Derwael, Lokeryggen and Hammarryggen Ice Rise records (Philippe and others, 2016; Wauthy and others, 2024; Wauthy and Dalaiden, 2026) are the only ice cores drilled at coastal ice rises in this region, but they are substantially farther east than our optimal sites. Goel and others (2020) evaluated the stability of ice rises in DML, which are promising ice core targets owing to their low ice velocity (Fig. 9b). Lyddan Ice Rise, located between the Brunt Ice Shelf and Riiser-Larsen Ice Shelf, stands out as the site which has the potential to constrain the most variance in annual Antarctic-wide temperature (Fig. 9a). Additionally, the 'double lineations', or double-peaked Raymond arches (Raymond, 1983), observed on Lyddan are an indicator of long-term stability (Goel and others, 2020). The Raymond arch suggests stability for the past ~3 ka and suggests deeper ice coring could also be of interest for longer temporal records. Furthermore, the regional accumulation signal from western DML is also of significant scientific interest, as increased snowfall in this region has been driving EAIS mass gain (Medley and others, 2018; Zuhr and others, 2026).

From a logistical perspective, Lyddan is also a feasible site. The accumulation rate is about 0.30 m a^{-1} ice equivalent (Table 1). Ice-penetrating radar data across Lyddan shows an accumulation gradient, with accumulation decreasing in the predominantly downwind (westward) direction (King and others, 2004), indicating snow redistribution by wind. Annual accumulation variations may be more difficult to distinguish from spatial variability because of the gradient, although temperature reconstructions should be less affected than accumulation. The existing radar profiles can be studied in detail for the purposes of site selection. Additionally, any proposal to drill at Lyddan should carefully analyze the potential for surface melting, which has been observed at nearby ice rises (Dey and others, 2023), as well as the impact of extreme precipitation events (Turner and others, 2019; Wauthy and Dalaiden, 2026). The British, Norwegian, Indian and Russian Antarctic programs are showing active interest in coastal DML ice drilling (e.g. Goel and others, 2025), and thus may be the best options for logistical support.

4.4 ITASE redrilling

The ITASE (Mayewski and others, 2005) collected a network of shallow (~50–300 m) ice cores from locations throughout Antarctica. The US-led portion collected many cores in the interior WAIS from 1999 to 2002 CE (Kaspari and others, 2004; Dixon and others, 2005; Steig and others, 2005, 2013; Banta and others, 2008; Schneider and Steig, 2008). These cores, and others in WAIS, have been highly effective at constraining 20th-century variability in annual West Antarctic accumulation (Fig. 3a and b, Fig. 4a and b). However, most of these records—with certain exceptions (e.g. Morris and others, 2017)—were drilled over two decades ago, which renders them unable to capture recent changes.

Initial efforts to drill shallow ice cores from coastal ice domes along the Amundsen Sea coast have been successful (Neff, 2020 and personal communication) and have the potential to improve projections of modern sea level change. However, the full potential of these new coastal records can only be realized if they are compared to records from inland WAIS, which are absent for the 21st-century. Updating the ITASE network would provide a continuous, high-resolution climate record that bridges the gap between past ice core data and ongoing satellite observations. This

Downloaded from https://www.cambridge.org/core. 15 Nov 2026 at 21:07:29, subject to the Cambridge Core terms of use.

extended overlap would improve calibration of remote sensing datasets, enhance detection of recent shifts in temperature and accumulation patterns, and refine projections of future ice sheet behavior under continued climate forcing.

In our redrilling tests, US-ITASE records in inland WAIS are consistently identified as optimal sites for constraining annual Antarctic-wide accumulation (Fig. 6a and b). In both climate models and reanalyses, accumulation from locations across western WAIS has high interannual covariance with Antarctic-wide accumulation (Fig. S1). The WAIS-EAIS, while geographic, is not necessarily climatological. Previous studies have found a climatological transition at approximately the East Antarctic Ice divide (~78° S–80° S) between predominantly Pacific-sourced and Indian-sourced air masses, where sites grid-west of the divide (e.g. South Pole, Kohnen) have a mean moisture source longitude of ~60° W to 180° W, associated with transport over WAIS and the Transantarctics (Sodemann and Stohl, 2009; Petteni and others, 2026). Thus, high-quality records from WAIS have the ability to provide information about accumulation variability in parts of EAIS.

In addition, sites in WAIS have a higher absolute accumulation rate, which we demonstrate generally correlates with higher annually resolved record quality due to lower timescale uncertainty in annual layer counting (Fig. 2). West Antarctic ice core records have also been found to show strong linkages to large-scale circulation signals (Küttel and others, 2012; Man and others, 2025), rendering them less susceptible to being dominated by stratigraphic noise and localized processes (e.g. wind-borne redistribution of snow). We further note that our results are reflective of our focus on interannual variability (more discussion in Section 4.5).

We seek to identify the most optimal drilling sites in WAIS. Similar to Fig. 7, we calculate an 'optimality score' for each US-ITASE site by adding in quadrature the normalized percent constrained variance from both the MME and MRE simulations (Fig. 10a). Two particular sites are identified as having the highest optimality scores: these are ITASE-1999-1 ('99-1') and ITASE-2001-2 ('01-2'). 99-1 is located in the vicinity of the Byrd camp, while 01-2 is about halfway between WAIS Divide and Hercules Dome.

Our analysis indicates that the information gained about annual Antarctic accumulation has diminishing returns after the first three records in West Antarctica are drilled (Fig. 10c). The 02-4 record (Jacobel and others, 2005) will be effectively updated with the uppermost part of the upcoming Hercules Dome ice core drilling (Fudge and others, 2023; Hills and others, 2025). Drilling three ~10–15-meter (~20–30 years) firn cores to update WAIS Divide, 99-1, and 01-2 would maximize the scientific return for the logistical effort. The drilling could be accomplished with day-long ground traverses or fixed-wing trips out of WAIS Divide. Both 99-1 and 01-2 are located approximately 250 km from WAIS Divide, with 99-1 being located close to the site of the former Byrd Camp, which has been proposed to (re-)replace WAIS Divide as the major West Antarctic logistical base for the United States Antarctic Program.

4.5 Outlook and future work

Our present ability to constrain the climate history of Antarctica is hampered by spatial and temporal limitations in the existing ice core network. The relative dearth of records in EAIS (Fig. 1a) has led to high uncertainties around historical Antarctic sea level contribution (Medley and Thomas, 2019; Eswaran and others, 2024); the slowed pace of ice core drilling since the 2000s means that our ability to reconstruct 21st-century annual temperature and accumulation is less than 10% that of the mid-20th century (Fig. 5).

Our data-driven optimal sensor methodology, already a well-established technique to identify paleoclimate observation sites (e.g. Comboul and others, 2015; Hakim and others, 2020), offers an objective way to evaluate future ice core sites. The three case studies above are intended as a demonstration of how our optimal sensor methodology can be combined with an evaluation of surface conditions and logistics to produce community-relevant drilling recommendations. Our study should not be taken as a formal recommendation to drill at these specific sites; rather, we use these case studies as illustrations that specific sites can be found within regions identified by the optimal sensor method. Here, we discuss the limitations in our specific implementation of the optimal sensor methodology, and potential avenues for future investigation. We emphasize that these limitations are not intrinsic to the optimal sensor approach as a concept, and can be mitigated by future work.

First, our temperature optimizations rely on the assumption that temperature scales linearly with $\delta^{18}O$. In reality, the relationship can be nonlinear, with dependencies on condensation and evaporation site temperatures and the deuterium excess parameter (Markle and Steig, 2022). In Antarctica, significant spatial and temporal variability has been observed in this relationship (Klein and others, 2019; Goursaud Oger and others, 2024). Thus, our proxy estimates are not perfect representations of $\delta^{18}O$ records, which lowers confidence in our identified optimal temperature sites. Nevertheless, we note that existing data assimilation-based polar climate reconstructions have predominantly used linear temperature-$\delta^{18}O$ calibration (e.g. Badgeley and others, 2020; O'Connor and others, 2021); furthermore, investigating the spatial correlations of reanalysis temperature fields is a well-established method of selecting ice core sites for water isotope records (e.g. Vance and others, 2016; Bertler and others, 2018). Future studies can use an isotope-enabled climate model (e.g. iCESM; Brady and others, 2019) or atmospheric reanalysis (e.g. WisoMIP; Bong and others, 2026) as the source ensemble of the proxy estimates; this would allow for direct assimilation of $\delta^{18}O$ records, which holds promise for skillful reconstruction of Antarctic temperature (Dalaiden and others, 2020). The climate ensemble can alternately be taken from high-resolution polar climate products (e.g. RACMO2; van Wessem and others, 2018). These regional climate products skillfully capture small-scale climate variations and surface processes, and would allow for a more targeted and localized selection of ice core sites.

Furthermore, our methodology relies on the assumption of stationarity; i.e. that the spatial covariance structure of the MME and MRE holds for the target reconstruction period. This assumption is not unique to our study, as it applies to any spatially complete Antarctic climate reconstruction using a model or reanalysis prior (e.g. Medley and Thomas, 2019). The MRE is particularly sensitive to shifts in atmospheric circulation induced by anthropogenic climate change; due to its short and modern timespan (1980–2019 CE), it may not effectively capture atmospheric circulation variability on decadal timescales. Recent reconstructions have indicated that dynamic, rather than thermodynamic, change is the primary driver of accumulation variability, which underscores the importance of atmospheric circulation (Medley and Thomas, 2019). Nevertheless, the limitations of the MRE are counterbalanced by

Downloaded from https://www.cambridge.org/core. 15 Nov 2026 at 21:07:29, subject to the Cambridge Core terms of use.

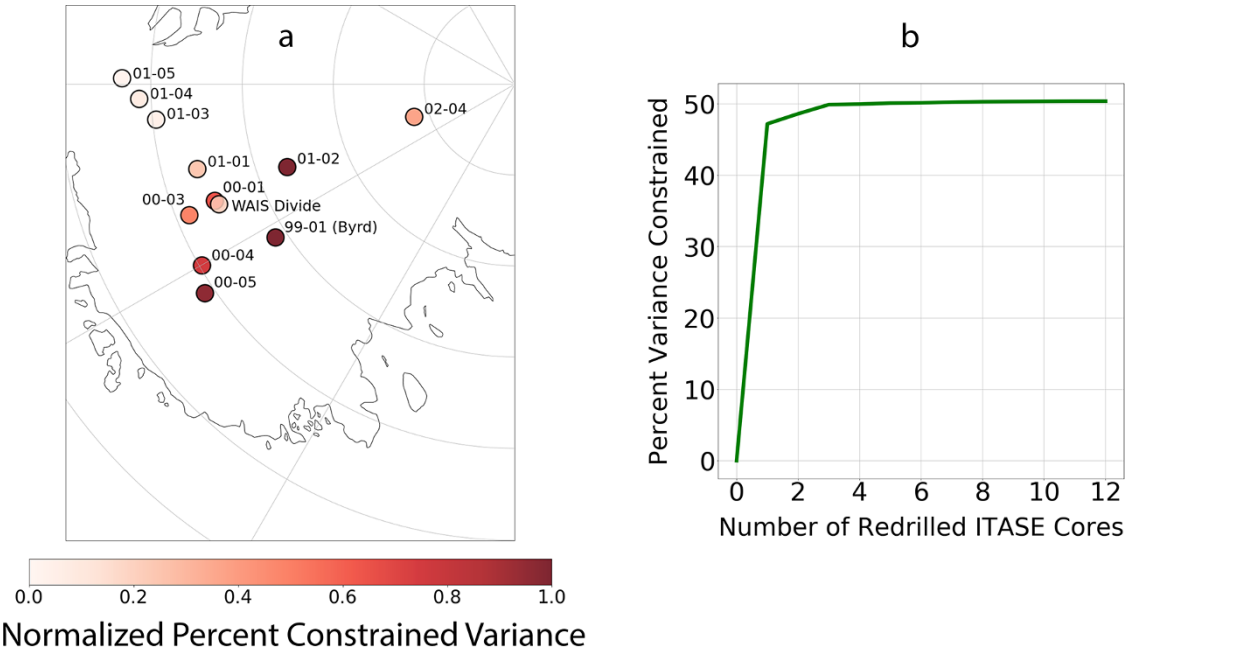


Figure 10. (a) Normalized percent of variance in annual Antarctic accumulation constrained by proxy estimates at ITASE coring sites sourced from the MME and MRE, combined in quadrature. (b) The percent variance constrained in annual Antarctic accumulation as a function of the number of hypothetically redrilled ITASE cores.

the MME, which is drawn from pre-anthropogenic (850–1850 CE) Last Millennium Simulations.

A separate direction for future investigation can be a more detailed examination of the spatial correlation length scale. Our results frequently find 'clusters' of adjacent optimal sites (Figs 3 and 4). It is true that a climate signal from a given region is certainly more robust given multiple records, as there always exists a timescale uncertainty in each record (quantified by the *R* value). Nevertheless, our methodology does not account for the fact that climate variability at adjacent sites will be dominated by the same synoptic-scale events (e.g. Vance and others, 2016), nor the spatial correlation in timescale uncertainty between adjacent records. Future work can adapt the optimal sensor algorithm to penalize the selection of closely adjacent sites, e.g. by adding a spatial correlation length scale cutoff or a different metric of distance.

Future studies can seek to better quantify the uncertainty in ice core records. Our accumulation rate-based estimate is a reasonable first-order approximation for the timescale uncertainty, but it does not objectively account for the numerous sources of spatial uncertainty (e.g. blowing snow, ice velocity and orographic variability) nor the impact of precipitation intermittency. Even at high-accumulation ice rise sites, these variables can create significant uncertainty in the record (e.g. Münch and Laepple, 2018). Incorporating these variables in an objective and quantitative fashion would lead to a stronger estimate of proxy uncertainty. Furthermore, hand-augured shallow cores offer a means of assessing the spatial representativeness of a given site.

In our study, we evaluated only the two climate metrics of annual continent-wide accumulation and temperature; future work can investigate different metrics for pertinent research questions. Other climate variables can be chosen, such as sea ice extent or atmospheric circulation indices including the Amundsen Sea Low (e.g. Raphael and others, 2016; O'Connor and others, 2025) and Southern Annual Mode (e.g. Marshall, 2003; O'Connor, Steig, Hakim, 2021; King and others, 2023b; Dalaiden and others, 2025). Alternatively, the optimal sensor algorithm can be adapted to optimize a vector, rather than a scalar metric (Hakim and others, 2020). This allows the algorithm to constrain spatial variability, rather than purely temporal variability, in the metric of interest. While our study primarily examines the variance constrained as a normalized value (Figs 3 and 4), the raw variance values can provide insight into reconstruction skill over time (Fig. 5) and into the optimal number of cores to drill (Fig. 10c).

Additionally, the climate metric can be optimized for subregions of Antarctica (e.g. the Ross Sea region), rather than for the entire AIS, WAIS or EAIS (e.g. Figs S3–S6). Our results show that the disaggregation of climate metrics into sub-regional estimates can lead to differing results, in addition to adding greater nuance to existing results. For example, the CIR region can constrain annual accumulation variability in both WAIS and EAIS (Fig. S3); the Lyddan Ice Rise region offers little insight into WAIS temperature, but is extremely well-placed to constrain EAIS temperature (Fig. S4). Regional disaggregation can identify new drilling locations that are not optimal for reconstructing a continental average; for example, coastal sites along the Amundsen and Bellingshausen Seas are not particularly optimal for the purposes of reconstructing annual AIS temperature, but are very well-placed to reconstruct annual WAIS temperature (Fig. S4). Performing additional experiments where the climate metric is disaggregated into smaller spatial regions, such as individual drainage basins, is a promising direction for future work.

While this study focuses on a specific temporal resolution, i.e. annually-resolved ice cores to reconstruct interannual variability for the past ~200 years, the presented methodology is equally applicable to other timescales of variability (e.g. decadal or centennial). We focus on interannual variability because it is well characterized in modern climatology; however, targeting a longer timescale could better utilize East Antarctic records, which do not resolve interannual variability due to low accumulation rates. Using

Downloaded from https://www.cambridge.org/core. 15 Nov 2026 at 21:07:29, subject to the Cambridge Core terms of use.

longer timescales will necessitate a new metric of proxy uncertainty; the uncertainty in annual layering becomes less important on lower-resolution timescales, while the spatial representation uncertainty due to ice flow becomes more important with longer timescales. This will increase the optimality of low-accumulation, low-ice velocity sites (e.g. ice domes on the East Antarctic Plateau). A longer-timescale optimal sensor analysis would rely solely on the MME, because the 40-year-long MRE is too short in duration to serve as a source of proxy estimates at these timescales.

An additional future application is to specifically reconstruct a continental metric rather than reconstructing histories for each grid cell and aggregating them. For past annual Antarctic accumulation, existing climate reconstructions have chosen to reconstruct each grid cell (e.g. Medley and Thomas, 2019; Dalaiden and others, 2021; Eswaran and others, 2024); continental-scale metrics are then calculated by spatially integrating across the grid cells. If the goal is to reconstruct the continental value, it may be more accurate and efficient to directly reconstruct the scalar metric, as this does not rely on the assumption of spatially homogeneous reconstruction skill (King and others, 2023a).

5. Conclusion

We present a novel data-driven approach to optimize the selection of Antarctic shallow ice-core sites for their ability to reconstruct annual Antarctic accumulation and average temperature at annual resolution since 1800. We choose two Antarctic-wide climate metrics to illustrate how the optimal sensor method can be used to guide ice-core site selection. The method is equally applicable for many other climate metrics, including regional reconstructions and other climate parameters. We account for dating and preservation uncertainty by scaling the uncertainty to the inverse of the accumulation rate. This enables us to produce a quantitative ranking of potential ice-core sites, to answer the pertinent questions of both 1) where to drill new records (to better constrain 19th–20th century climate variability) and 2) where to redrill old records (to extend their chronologies into the 21st-century).

We find that the southern end of the Ross Ice Shelf is the best drilling region for reconstructing annual Antarctic accumulation (Fig. 7b), while the west coast of DML is the best region to reconstruct annual Antarctic temperature (Fig. 7c). We recognize that the optimal sensor algorithm cannot capture all the relevant complexities of ice-core site selection, so we present three 'case studies' to investigate the feasibility of these sites: 1) new drilling at CIR, 2) new drilling at Lyddan Ice Rise, and 3) redrilling the US-ITASE cores. Crary and Lyddan Ice Rises are logistically feasible to access and have existing ice-penetrating radar profiles, which allow for more precise selection of drilling sites. For the redrilling of the US-ITASE cores, we find that redrilling three records is the best trade-off between maximizing climate reconstruction skill and minimizing the logistical burden. In a broader sense, there is a compelling need to update the Antarctic ice-core network, particularly as the pace of drilling has slowed in recent decades. New records would place recent mass change in a historical context, and would extend the overlap period with satellite-era reanalysis. This paper offers a data-driven approach to optimize site selection and provides an objective means to answer the question of where to drill ice cores for reconstructing any climate metric of choice.

Supplementary material. The supplementary material for this article can be found at https://doi.org/10.1017/jog.2026.10218.

Data availability statement. The results of our experiments can be found on Zenodo at https://doi.org/10.5281/zenodo.21523198. The code used to reproduce our results can be found at https://github.com/advikeswaran/optimal-sensor. The optimal sensor analyses were conducted using the DASH open-source data assimilation framework (King and others, 2023a). Positions of the ice-core sites were taken from the PAGES Antarctica 2k records (Stenni and others, 2017; Thomas and others, 2017), with some additions (Criscitiello and others, 2013; Medley and others, 2013, 2018; Philippe and others, 2016; Kahle and others, 2021). The MME was constructed using CMIP5 Last Millennium simulations (Collins and others, 2001; Gent and others, 2011; Phipps and others, 2012; Bao and others, 2013; Dufresne and others, 2013; Schmidt and others, 2014; Wu and others, 2014; Brady and others, 2019; Gutjahr and others, 2019). The MRE was constructed using four reanalyses: ERA5 (Hersbach and others, 2020), MERRA-2 (Gelaro and others, 2017), CFSR (Saha and others, 2014) and JRA-55 (Kobayashi and others, 2015). For the case studies, data are qualitatively analyzed from ice-penetrating radar at Crary Ice Rise (Hillebrand and others, 2021) and Lyddan Ice Rise (King and others, 2004), as well as the US-ITASE ice cores in West Antarctica (Kaspari and others, 2004; Dixon and others, 2005; Banta and others, 2008; Steig and others, 2013).

Acknowledgements. We thank Mathieu Casado (scientific editor) and four anonymous reviewers for their constructive feedback and improvements to the manuscript. We thank Jonathan King for providing the open-source code framework (DASH) used to implement the optimal sensor algorithm. The PAGES Antarctica2k and CMIP initiatives, along with reanalyses developed by ECMWF, NASA, NOAA and JMA, provided the compilation of original data sources for this study. We thank the ITASE initiative for originally identifying, drilling and analyzing cores from many of the sites examined in this study. We thank Michael Town and members of the University of Washington Glaciology group for fruitful discussions. A.E. was supported by funding from the University of Washington Program on Climate Change. Travel funding for A.E. was supported by the Princeton University Office of Undergraduate Research. O.J.T., S.M. and V.H.L.W. were supported by the New Zealand Ministry of Business, Innovation and Employment through the Antarctic Science Platform (ANTARCTICANZ2504). V.H.L.W. was supported by a Rutherford Discovery Fellowship awarded by the Royal Society Te Apārangi from New Zealand Government funding (RDF-VUW2203).

Author contributions. A.E., O.J.T. and T.J.F. conceptualized the project. A.E. performed all the experiments and data analysis in this study, and prepared the original draft of the manuscript. O.J.T. and T.J.F. were the primary supervisors of this study and guided the design of the methodology and the interpretation of the results. O.J.T., S.M., K.M., P.D.N., E.J.S., V.H.L.W. and T.J.F. provided feedback on the draft and guided the formulation of the case studies.

References

Alley RB and 11 others (1997) Visual-stratigraphic dating of the GISP2 ice core: Basis, reproducibility, and application. *Journal of Geophysical Research: Oceans* **102**(C12), 26367–26381. doi: 10.1029/96JC03837.

Badgeley JA, Steig EJ, Hakim GJ and Fudge TJ (2020) Greenland temperature and precipitation over the last 20,000 years using data assimilation. *Climate of the Past* **16**(4), 1325–1346. doi: 10.5194/cp-16-1325-2020.

Banta JR, McConnell JR, Frey MM, Bales RC and Taylor K (2008) Spatial and temporal variability in snow accumulation at the West Antarctic Ice Sheet Divide over recent centuries. *Journal of Geophysical Research: Atmospheres* **113**(D23). doi: 10.1029/2008JD010235.

Bao Q and 12 others (2013) The flexible global ocean-atmosphere-land system model, spectral version 2: FGOALS-s2. *Advances in Atmospheric Sciences* **30**(3), 561–576. doi: 10.1007/s00376-012-2113-9.

Bertler NAN and 19 others (2018) The Ross Sea Dipole – Temperature, snow accumulation and sea ice variability in the Ross Sea region, Antarctica, over the past 2700 years. *Climate of the Past* **14**(2), 193–214. doi: 10.5194/cp-14-193-2018.

Bindschadler RA, Roberts EP and Iken A (1990) Age of Crary Ice Rise, Antarctica, determined from temperature-depth profiles. *Annals of Glaciology* **14**, 13–16. doi: 10.3189/S0260305500008168.

Downloaded from https://www.cambridge.org/core. 15 Nov 2026 at 21:07:29, subject to the Cambridge Core terms of use.

Boisvert LN, Webster MA, Petty AA, Markus T, Bromwich DH and Cullather RI (2018) Intercomparison of precipitation estimates over the Arctic Ocean and its peripheral seas from reanalyses. *Journal of Climate* **31**(20), 8441–8462. doi: 10.1175/JCLI-D-18-0125.1.

Bong H and 19 others (2026) Water Isotope Model Intercomparison Project (WisoMIP): Present-day Climate. *Journal of Geophysical Research: Atmospheres* **131**, e2025JD044985. doi: 10.1029/2025JD044985.

Brady E and 11 others (2019) The connected isotopic water cycle in the community earth system model version 1. *Journal of Advances in Modeling Earth Systems* **11**(8), 2547–2566. doi: 10.1029/2019MS001663.

Bromwich DH (1988) Snowfall in high southern latitudes. *Reviews of Geophysics* **26**(1), 149–168. doi: 10.1029/RG026i001p00149.

Bromwich DH, Ensign A, Wang S-H and Zou X (2024) Major artifacts in ERA5 2-m sr Antarctica prior to and during the modern satellite era. *Geophysical Research Letters* **51**(21), e2024GL111907. doi: 10.1029/2024GL111907.

Bromwich DH, Fogt RL, Hodges KI and Walsh JE (2007) A tropospheric assessment of the ERA-40, NCEP, and JRA-25 global reanalyses in the polar regions. *Journal of Geophysical Research: Atmospheres* **112**(D10). doi: 10.1029/2006JD007859.

Bromwich DH, Nicolas JP and Monaghan AJ (2011) An assessment of precipitation changes over Antarctica and the southern ocean since 1989 in contemporary global reanalyses. *Journal of Climate* **24**(16), 4189–4209. doi: 10.1175/2011JCLI4074.1.

Bumbaco KA, Hakim GJ, Mauger GS, Hryniw N and Steig EJ (2014) Evaluating the Antarctic observational network with the Antarctic Mesoscale Prediction System (AMPS). *Monthly Weather Review* **142**(10), 3847–3859. doi: 10.1175/MWR-D-13-00401.1.

Casado M, Münch T and Laepple T (2020) Climatic information archived in ice cores: Impact of intermittency and diffusion on the recorded isotopic signal in Antarctica. *Climate of the Past* **16**(4), 1581–1598. doi: 10.5194/cp-16-1581-2020.

Catania G, Hulbe C, Conway H, Scambos TA and Raymond CF (2012) Variability in the mass flux of the Ross ice streams, West Antarctica, over the last millennium. *Journal of Glaciology* **58**(210), 741–752. doi: 10.3189/2012JoG11J219.

Cavitte MGP and 9 others (2023) Investigating the spatial representativeness of East Antarctic ice cores: A comparison of ice core and radar-derived surface mass balance over coastal ice rises and Dome Fuji. *The Cryosphere* **17**(11), 4779–4795. doi: 10.5194/tc-17-4779-2023.

Collins M, Tett SFB and Cooper C (2001) The internal climate variability of HadCM3, a version of the Hadley Centre coupled model without flux adjustments. *Climate Dynamics* **17**(1), 61–81. doi: 10.1007/s003820000094.

Comboul M, Emile-Geay J, Hakim GJ and Evans MN (2015) Paleoclimate sampling as a sensor placement problem. *Journal of Climate* **28**(19), 7717–7740. doi: 10.1175/JCLI-D-14-00802.1.

Criscitiello AS and 7 others (2013) Ice sheet record of recent sea-ice behavior and polynya variability in the Amundsen Sea, West Antarctica. *Journal of Geophysical Research: Oceans* **118**(1), 118–130. doi: 10.1029/2012JC008077.

Cuffey KM and Steig EJ (1998) Isotopic diffusion in polar firn: Implications for interpretation of seasonal climate parameters in ice-core records, with emphasis on central Greenland. *Journal of Glaciology* **44**(147), 273–284. doi: 10.3189/S0022143000002616.

Curran MAJ, Van Ommen TD and Morgan V (1998) Seasonal characteristics of the major ions in the high-accumulation Dome Summit South ice core, Law Dome, Antarctica. *Annals of Glaciology* **27**, 385–390. doi: 10.3189/1998AoG27-1-385-390.

Dalaiden Q, Goosse H, Holland PR and Barthelemy A (2025) Dynamical reconstruction of Southern Ocean and Antarctic climate variability since 1700. *Scientific Data* **12**(1), 1574. doi: 10.1038/s41597-025-05808-w.

Dalaiden Q and 6 others (2020) How useful is snow accumulation in reconstructing surface air temperature in Antarctica? A study combining ice core records and climate models. *The Cryosphere* **14**(4), 1187–1207. doi: 10.5194/tc-14-1187-2020.

Dalaiden Q, Goosse H, Rezsöhazy J and Thomas ER (2021) Reconstructing atmospheric circulation and sea-ice extent in the West Antarctic over the past 200 years using data assimilation. *Climate Dynamics* **57**(11), 3479–3503. doi: 10.1007/s00382-021-05879-6.

Dale ER, McDonald AJ, Coggins JHJ and Rack W (2017) Atmospheric forcing of sea ice anomalies in the Ross Sea polynya region. *The Cryosphere* **11**(1), 267–280. doi: 10.5194/tc-11-267-2017.

Dee SG, Steiger NJ, Emile-Geay J and Hakim GJ (2016) On the utility of proxy system models for estimating climate states over the common era. *Journal of Advances in Modeling Earth Systems* **8**(3), 1164–1179. doi: 10.1002/2016MS000677.

Dey R and 6 others (2023) Application of visual stratigraphy from line-scan images to constrain chronology and melt features of a firn core from coastal Antarctica. *Journal of Glaciology* **69**(273), 179–190. doi: 10.1017/jog.2022.59.

Dixon D and 7 others (2005) A 200 year sulfate record from 16 Antarctic ice cores and associations with Southern Ocean sea-ice extent. *Annals of Glaciology* **41**, 155–166. doi: 10.3189/172756405781813366.

Dufresne J-L and 19 others (2013) Climate change projections using the IPSL-CM5 Earth System Model: From CMIP3 to CMIP5. *Climate Dynamics* **40**(9), 2123–2165. doi: 10.1007/s00382-012-1636-1.

Edwards TL and 19 others (2021) Projected land ice contributions to twenty-first-century sea level rise. *Nature* **593**(7857), 74–82. doi: 10.1038/s41586-021-03302-y.

Eswaran A, Truax OJ and Fudge TJ (2024) 20th-Century Antarctic Sea level mitigation driven by uncertain East Antarctic accumulation history. *Geophysical Research Letters* **51**(9), e2023GL106991. doi: 10.1029/2023GL106991.

Frieler K and 8 others (2015) Consistent evidence of increasing Antarctic accumulation with warming. *Nature Climate Change* **5**(4), 348–352. doi: 10.1038/nclimate2574.

Fudge TJ and 9 others (2023) A site for deep ice coring at West Hercules dome: Results from ground-based geophysics and modeling. *Journal of Glaciology* **69**(275), 538–550. doi: 10.1017/jog.2022.80.

Fudge TJ and 8 others (2016) Variable relationship between accumulation and temperature in West Antarctica for the past 31,000 years. *Geophysical Research Letters* **43**(8), 3795–3803. doi: 10.1002/2016GL068356.

Gelaro R and 19 others (2017) The modern-era retrospective analysis for research and applications, version 2 (MERRA-2). *Journal of Climate* **30**(14), 5419–5454. doi: 10.1175/JCLI-D-16-0758.1.

Gent PR and 12 others (2011) The community climate system model version 4. *Journal of Climate* **24**(19), 4973–4991. doi: 10.1175/2011JCLI4083.1.

Goel V and 7 others (2025) A new coastal ice-core site identified in dronning maud land, Antarctica, for high-resolution climate reconstructions to the Last Glacial Maximum. *EGUsphere* **2025**, 1–28. doi: 10.5194/egusphere-2025-2037.

Goel V, Matsuoka K, Berger CD, Lee I, Dall J and Forsberg R (2020) Characteristics of ice rises and ice rumples in Dronning Maud Land and Enderby Land, Antarctica. *Journal of Glaciology* **66**(260), 1064–1078. doi: 10.1017/jog.2020.77.

Goodwin BP, Mosley-Thompson E, Wilson AB, Porter SE and Sierra-Hernandez MR (2016) Accumulation variability in the Antarctic Peninsula: The role of large-scale atmospheric oscillations and their interactions. *Journal of Climate* **29**(7), 2579–2596. doi: 10.1175/JCLI-D-15-0354.1.

Goosse H and 12 others (2012) Antarctic temperature changes during the last millennium: Evaluation of simulations and reconstructions. *Quaternary Science Reviews* **55**, 75–90. doi: 10.1016/j.quascirev.2012.09.003.

Goosse H, Crespin E, de Montety A, Mann ME, Renssen H and Timmermann A (2010) Reconstructing surface temperature changes over the past 600 years using climate model simulations with data assimilation. *Journal of Geophysical Research: Atmospheres* **115**(D9). doi: 10.1029/2009JD012737.

Goursaud Oger S, Sime LC and Holloway M (2024) Decoupling of $\delta^{18}O$ from surface temperature in Antarctica in an ensemble of historical simulations. *Climate of the Past* **20**(11), 2539–2560. doi: 10.5194/cp-20-2539-2024.

Gutjahr O and 7 others (2019) Max planck institute earth system model (MPI-ESM1.2) for the high-resolution model intercomparison project (HighResMIP). *Geoscientific Model Development* **12**(7), 3241–3281. doi: 10.5194/gmd-12-3241-2019.

Downloaded from https://www.cambridge.org/core. 15 Nov 2026 at 21:07:29, subject to the Cambridge Core terms of use.

Hakim GJ, Bumbaco KA, Tardif R and Powers JG (2020) Optimal network design applied to monitoring and forecasting surface temperature in Antarctica. *Monthly Weather Review* **148**(2), 857–873. doi: 10.1175/MWR-D-19-0103.1.

Hakim GJ and 7 others (2016) The last millennium climate reanalysis project: Framework and first results. *Journal of Geophysical Research: Atmospheres* **121**(12), 6745–6764. doi: 10.1002/2016JD024751.

Hersbach H and 19 others (2020) The ERA5 global reanalysis. *Quarterly Journal of the Royal Meteorological Society* **146**(730), 1999–2049. doi: 10.1002/qj.3803.

Hillebrand TR, Conway H, Koutnik M, Martín C, Paden J and Winberry JP (2021) Radio-echo sounding and waveform modeling reveal abundant marine ice in former rifts and basal crevasses within Crary Ice Rise, Antarctica. *Journal of Glaciology* **67**(264), 641–652. doi: 10.1017/jog.2021.17.

Hills BH and 8 others (2025) Radar-derived crystal orientation fabric suggests dynamic stability at the summit of hercules dome. *Journal of Geophysical Research: Earth Surface* **130**(3), e2023JF007588. doi: 10.1029/2023JF007588.

Hoffmann HM and 6 others (2022) The ST22 chronology for the skytrain ice rise ice core – Part 1: A stratigraphic chronology of the last 2000 years. *Climate of the Past* **18**(8), 1831–1847. doi: 10.5194/cp-18-1831-2022.

Hoffmann-Abdi K and 8 others (2023) Deciphering stable water isotope records of firn cores from a strongly maritime, high-accumulation site on the Antarctic Peninsula. *Journal of Glaciology* **69**(278), 2027–2045. doi: 10.1017/jog.2023.79.

Jackson SL, Vance TR, Crockart C, Moy A, Plummer C and Abram NJ (2023) Climatology of the Mount Brown South ice core site in East Antarctica: Implications for the interpretation of a water isotope record. *Climate of the Past* **19**(8), 1653–1675. doi: 10.5194/cp-19-1653-2023.

Jacobel RW, Welch BC, Steig EJ and Schneider DP (2005) Glaciological and climatic significance of Hercules Dome, Antarctica: An optimal site for deep ice core drilling. *Journal of Geophysical Research: Earth Surface* **110**(F1). doi: 10.1029/2004JF000188.

Kahle EC and 13 others (2021) Reconstruction of temperature, accumulation rate, and layer thinning from an ice core at South Pole, using a statistical inverse method. *Journal of Geophysical Research: Atmospheres* **126**(13), e2020JD033300. doi: 10.1029/2020JD033300.

Kaspari S and 6 others (2004) Climate variability in West Antarctica derived from annual accumulation-rate records from ITASE firn/ice cores. *Annals of Glaciology* **39**, 585–594. doi: 10.3189/172756404781814447.

King J, Anchukaitis KJ, Allen K, Vance T and Hessl A (2023b) Trends and variability in the Southern Annular Mode over the Common Era. *Nature Communications* **14**(1), 2324. doi: 10.1038/s41467-023-37643-1.

King J, Tierney J, Osman M, Judd EJ and Anchukaitis KJ (2023a) DASH: A MATLAB toolbox for paleoclimate data assimilation. *Geoscientific Model Development* **16**(19), 5653–5683. doi: 10.5194/gmd-16-5653-2023.

King JC, Anderson PS, Vaughan DG, Mann GW, Mobbs SD and Vosper SB (2004) Wind-borne redistribution of snow across an Antarctic ice rise. *Journal of Geophysical Research: Atmospheres* **109**(D11). doi: 10.1029/2003JD004361.

Klein F and 12 others (2019) Assessing the robustness of Antarctic temperature reconstructions over the past 2 millennia using pseudoproxy and data assimilation experiments. *Climate of the Past* **15**(2), 661–684. doi: 10.5194/cp-15-661-2019.

Kobayashi S and 12 others (2015) The JRA-55 Reanalysis: General specifications and basic characteristics. *Journal of the Meteorological Society of Japan Series II* **93**(1), 5–48. doi: 10.2151/jmsj.2015-001.

Koutnik MR and 7 others (2016) Holocene accumulation and ice flow near the West Antarctic Ice Sheet Divide ice core site. *Journal of Geophysical Research: Earth and Surface* **121**(5), 907–924. doi: 10.1002/2015JF003668.

Küttel M, Steig EJ, Ding Q, Monaghan AJ and Battisti DS (2012) Seasonal climate information preserved in West Antarctic ice core water isotopes: Relationships to temperature, large-scale circulation, and sea ice. *Climate Dynamics* **39**(7), 1841–1857. doi: 10.1007/s00382-012-1460-7.

Lenaerts JTM, Medley B, van den Broeke MR and Wouters B (2019) Observing and modeling ice sheet surface mass balance. *Reviews of Geophysics* **57**(2), 376–420. doi: 10.1029/2018RG000622.

Lenaerts JTM, Vizcaino M, Fyke J, van Kampenhout L and van den Broeke MR (2016) Present-day and future Antarctic ice sheet climate and surface mass balance in the Community Earth System Model. *Climate Dynamics* **47**(5), 1367–1381. doi: 10.1007/s00382-015-2907-4.

MacAyeal DR, Bindschadler RA, Shabtaie S, Stephenson S and Bentley CR (1987) Force, mass, and energy budgets of the Crary Ice Rise Complex, Antarctica. *Journal of Glaciology* **33**(114), 218–230. doi: 10.3189/S0022143000008728.

Man K and 10 others (2025) Century-long West Antarctic snow accumulation changes induced by tropical teleconnections. *Science Advances* **11**(5), eadr2821. doi: 10.1126/sciadv.adr2821.

Markle BR, Bertler NAN, Sinclair KE and Sneed SB (2012) Synoptic variability in the Ross Sea region, Antarctica, as seen from back-trajectory modeling and ice core analysis. *Journal of Geophysical Research: Atmospheres* **117**(D2). doi: 10.1029/2011JD016437.

Markle BR and Steig EJ (2022) Improving temperature reconstructions from ice-core water-isotope records. *Climate of the Past* **18**(6), 1321–1368. doi: 10.5194/cp-18-1321-2022.

Marshall GJ (2003) Trends in the Southern Annular mode from observations and reanalyses. *Journal of Climate* **16**(24), 4134–4143. doi: 10.1175/1520-0442(2003)016<4134:TITSAM>2.0.CO;2.

Matsuoka K and 19 others (2015) Antarctic ice rises and rumples: Their properties and significance for ice-sheet dynamics and evolution. *Earth-Science Reviews* **150**, 724–745. doi: 10.1016/j.earscirev.2015.09.004.

Mauger GS, Bumbaco KA, Hakim GJ and Mote PW (2013) Optimal design of a climatological network: Beyond practical considerations. *Geoscientific Instrumentation, Methods and Data Systems* **2**(2), 199–212. doi: 10.5194/gi-2-199-2013.

Mayewski PA and 18 others (2005) The International Trans-Antarctic Scientific Expedition (ITASE): An overview. *Annals of Glaciology* **41**, 180–185. doi: 10.3189/172756405781813159.

Medley B and 12 others (2013) Airborne-radar and ice-core observations of annual snow accumulation over Thwaites Glacier, West Antarctica confirm the spatiotemporal variability of global and regional atmospheric models. *Geophysical Research Letters* **40**(14), 3649–3654. doi: 10.1002/grl.50706.

Medley B and 12 others (2018) Temperature and snowfall in western Queen Maud Land increasing faster than climate model projections. *Geophysical Research Letters* **45**(3), 1472–1480. doi: 10.1002/2017GL075992.

Medley B and Thomas ER (2019) Increased snowfall over the Antarctic Ice Sheet mitigated twentieth-century sea-level rise. *Nature Climate Change* **9**(1), 34–39. doi: 10.1038/s41558-018-0356-x.

Monaghan AJ and 15 others (2006) Insignificant change in Antarctic Snowfall since the international geophysical year. *Science* **313**(5788), 827–831. doi: 10.1126/science.1128243.

Monnin E and 12 others (2004) Evidence for substantial accumulation rate variability in Antarctica during the Holocene, through synchronization of CO2 in the Taylor Dome, Dome C and DML ice cores. *Earth and Planetary Science Letters* **224**(1), 45–54. doi: 10.1016/j.epsl.2004.05.007.

Morlighem M and 19 others (2020) Deep glacial troughs and stabilizing ridges unveiled beneath the margins of the Antarctic ice sheet. *Nature Geoscience* **13**(2), 132–137. doi: 10.1038/s41561-019-0510-8.

Morris EM and 9 others (2017) Snow densification and recent accumulation along the iSTAR traverse, Pine Island Glacier, Antarctica. *Journal of Geophysical Research: Earth Surface* **122**(12), 2284–2301. doi: 10.1002/2017JF004357.

Mottram R and 16 others (2021) What is the surface mass balance of Antarctica? An intercomparison of regional climate model estimates. *The Cryosphere* **15**(8), 3751–3784. doi: 10.5194/tc-15-3751-2021.

Mulvaney R and 8 others (2002) 1000 year ice-core records from Berkner Island, Antarctica. *Annals of Glaciology* **35**, 45–51. doi: 10.3189/172756402781817176.

Münch T and Laepple T (2018) What climate signal is contained in decadal- to Centennial-scale isotope variations from Antarctic ice cores? *Climate of the Past* **14**(12), 2053–2070. doi: 10.5194/cp-14-2053-2018.

Neff PD (2020) Amundsen Sea coastal ice rises: Future sites for marine-focused ice core records. *Oceanography* **33**(2), 88–89. doi: 10.5670/oceanog.2020.215.

Downloaded from https://www.cambridge.org/core. 15 Nov 2026 at 21:07:29, subject to the Cambridge Core terms of use.

Nicola L, Notz D and Winkelmann R (2023) Revisiting temperature sensitivity: How does Antarctic precipitation change with temperature? *The Cryosphere* **17**(7), 2563–2583. doi: 10.5194/tc-17-2563-2023.

O'Connor GK and 7 others (2025) Enhanced West Antarctic ice loss triggered by polynya response to meridional winds. *Nature Geoscience* **18**(9), 840–847. doi: 10.1038/s41561-025-01757-6.

O'Connor GK, Steig EJ and Hakim GJ (2021) Strengthening southern hemisphere westerlies and Amundsen Sea low deepening over the 20th century revealed by proxy-data assimilation. *Geophysical Research Letters* **48**(24), e2021GL095999. doi: 10.1029/2021GL095999.

O'Neill JF and 8 others (2025) ISMIP6-based Antarctic projections to 2100: Simulations with the BISICLES ice sheet model. *The Cryosphere* **19**(2), 541–563. doi: 10.5194/tc-19-541-2025.

Oerter H, Graf W, Wilhelms F, Minikin A and Miller H (1999) Accumulation studies on Amundsenisen, Dronning Maud Land, Antarctica, by means of tritium, dielectric profiling and stable-isotope measurements: First results from the 1995–96 and 1996–97 field seasons. *Annals of Glaciology* **29**, 1–9. doi: 10.3189/172756499781820914.

Orsi AJ, Cornuelle BD and Severinghaus JP (2012) Little Ice Age cold interval in West Antarctica: Evidence from borehole temperature at the West Antarctic Ice Sheet (WAIS) Divide. *Geophysical Research Letters* **39**(9). doi: 10.1029/2012GL051260.

Orsi AJ, Kawamura K, Fegyveresi JM, Headly MA, Alley RB and Severinghaus JP (2015) Differentiating bubble-free layers from melt layers in ice cores using noble gases. *Journal of Glaciology* **61**(227), 585–594. doi: 10.3189/2015JoG14J237.

Palerme C, Genthon C, Claud C, Kay JE, Wood NB and L'ecuyer T (2017) Evaluation of current and projected Antarctic precipitation in CMIP5 models. *Climate Dynamics* **48**(1), 225–239. doi: 10.1007/s00382-016-3071-1.

Parsons LA, Amrhein DE, Sanchez SC, Tardif R, Brennan MK and Hakim GJ (2021) Do multi-model ensembles improve reconstruction skill in paleoclimate data assimilation? *Earth and Space Science* **8**(4), e2020EA001467. doi: 10.1029/2020EA001467.

Patterson MO and 19 others (2022) Sensitivity of the West Antarctic Ice Sheet to +2 °C (SWAIS 2C). *Scientific Drilling* **30**, 101–112. doi: 10.5194/sd-30-101-2022.

Payne AJ and 19 others (2021) Future sea level change under coupled model intercomparison project phase 5 and phase 6 scenarios from the Greenland and Antarctic s. *Geophysical Research Letters* **48**(16), e2020GL091741. doi: 10.1029/2020GL091741.

Petteni A and 10 others (2026) Air mass origin and local impacts on Antarctic snow isotopic composition: An observation and modelling study. *The Cryosphere* **20**(6), 3581–3598. doi: 10.5194/tc-20-3581-2026.

Philippe M and 10 others (2016) Ice core evidence for a 20th century increase in surface mass balance in coastal Dronning Maud Land, East Antarctica. *The Cryosphere* **10**(5), 2501–2516. doi: 10.5194/tc-10-2501-2016.

Phipps SJ, Rotstayn LD, Gordon HB, Roberts JL, Hirst AC and Budd WF (2012) The CSIRO Mk3L climate system model version 1.0 – Part 2: Response to external forcings. *Geoscientific Model Development* **5**(3), 649–682. doi: 10.5194/gmd-5-649-2012.

Raphael MN and 8 others (2016) The Amundsen Sea low: Variability, change, and impact on Antarctic climate. *Bulletin of the American Meteorological Society* **97**(1), 111–121. doi: 10.1175/BAMS-D-14-00018.1.

Raymond CF (1983) Deformation in the vicinity of ice divides. *Journal of Glaciology* **29**(103), 357–373. doi: 10.3189/S0022143000030288.

Rhodes RH and 8 others (2012) Little Ice Age climate and oceanic conditions of the Ross Sea, Antarctica from a coastal ice core record. *Climate of the Past* **8**(4), 1223–1238. doi: 10.5194/cp-8-1223-2012.

Rignot E, Mouginot J, Scheuchl B and Jeong S (2022) Changes in Antarctic ice sheet motion derived from satellite radar interferometry between 1995 and 2022. *Geophysical Research Letters* **49**(23), e2022GL100141. doi: 10.1029/2022GL100141.

Rignot E, Mouginot J, Scheuchl B, van den Broeke M, van Wessem MJ and Morlighem M (2019) Four decades of Antarctic Ice Sheet mass balance from 1979–2017. *Proceedings of the National Academy of Sciences* **116**(4), 1095–1103. doi: 10.1073/pnas.1812883116.

Saha S and 18 others (2014) The NCEP climate forecast system version 2. *Journal of Climate* **27**(6), 2185–2208. doi: 10.1175/JCLI-D-12-00823.1.

Schmidt GA and 19 others (2014) Configuration and assessment of the GISS ModelE2 contributions to the CMIP5 archive. *Journal of Advances in Modeling Earth Systems* **6**(1), 141–184. doi: 10.1002/2013MS000265.

Schneider DP and Fogt RL (2018) Artifacts in century-length atmospheric and coupled reanalyses over Antarctica due to historical data availability. *Geophysical Research Letters* **45**(2), 964–973. doi: 10.1002/2017GL076226.

Schneider DP and Steig EJ (2008) Ice cores record significant 1940s Antarctic warmth related to tropical climate variability. *Proceedings of the National Academy of Sciences* **105**(34), 12154–12158. doi: 10.1073/pnas.0803627105.

Schneider DP and 6 others (2006) Antarctic temperatures over the past two centuries from ice cores. *Geophysical Research Letters* **33**(16). doi: 10.1029/2006GL027057.

Seroussi H and 12 others (2024) Evolution of the Antarctic Ice Sheet over the next three centuries from an ISMIP6 model ensemble. *Earth's Future* **12**(9), e2024EF004561. doi: 10.1029/2024EF004561.

Servettaz APM and 10 others (2020) Snowfall and water stable isotope variability in East Antarctica controlled by warm synoptic events. *Journal of Geophysical Research: Atmospheres* **125**(17), e2020JD032863. doi: 10.1029/2020JD032863.

Smith B and 14 others (2020) Pervasive ice sheet mass loss reflects competing ocean and atmosphere processes. *Science* **368**(6496), 1239–1242. doi: 10.1126/science.aaz5845.

Sodemann H and Stohl A (2009) Asymmetries in the moisture origin of Antarctic precipitation. *Geophysical Research Letters* **36**(22). doi: 10.1029/2009GL040242.

Stauffer B, Flückiger J, Wolff E and Barnes P (2004) The EPICA deep ice cores: First results and perspectives. *Annals of Glaciology* **39**, 93–100. doi: 10.3189/172756404781814500.

Steig EJ and 19 others (2013) Recent climate and ice-sheet changes in West Antarctica compared with the past 2,000 years. *Nature Geoscience* **6**(5), 372–375. doi: 10.1038/ngeo1778.

Steig EJ and 15 others (2005) High-resolution ice cores from US ITASE (West Antarctica): Development and validation of chronologies and determination of precision and accuracy. *Annals of Glaciology* **41**, 77–84. doi: 10.3189/172756405781813311.

Steig EJ, Schneider DP, Rutherford SD, Mann ME, Comiso JC and Shindell DT (2009) Warming of the Antarctic ice-sheet surface since the 1957 International geophysical year. *Nature* **457**(7228), 459–462. doi: 10.1038/nature07669.

Steiger NJ, Hakim GJ, Steig EJ, Battisti DS and Roe GH (2014) Assimilation of time-averaged pseudoproxies for climate reconstruction. *Journal of Climate* **27**(1), 426–441. doi: 10.1175/JCLI-D-12-00693.1.

Steiger NJ, Steig EJ, Dee SG, Roe GH and Hakim GJ (2017) Climate reconstruction using data assimilation of water isotope ratios from ice cores. *Journal of Geophysical Research: Atmospheres* **122**(3), 1545–1568. doi: 10.1002/2016JD026011.

Stenni B and 8 others (1999) 200 years of isotope and chemical records in a firn core from Hercules Névé, northern Victoria Land, Antarctica. *Annals of Glaciology* **29**, 106–112. doi: 10.3189/172756499781821175.

Stenni B and 17 others (2017) Antarctic climate variability on regional and continental scales over the last 2000 years. *Climate of the Past* **13**(11), 1609–1634. doi: 10.5194/cp-13-1609-2017.

Tang MSY, Chenoli SN, Samah AA and Hai OS (2018) An assessment of historical Antarctic precipitation and temperature trend using CMIP5 models and reanalysis datasets. *Polar Science* **15**, 1–12. doi: 10.1016/j.polar.2018.01.001.

Tardif R and 8 others (2019) Last Millennium Reanalysis with an expanded proxy database and seasonal proxy modeling. *Climate of the Past* **15**(4), 1251–1273. doi: 10.5194/cp-15-1251-2019.

Taylor KC and 13 others (2004) Dating the Siple Dome (Antarctica) ice core by manual and computer interpretation of annual layering. *Journal of Glaciology* **50**(170), 453–461. doi: 10.3189/172756504781829864.

Thamban M, Laluraj CM, Naik SS and Chaturvedi A (2011) Reconstruction of Antarctic climate change using ice core proxy records from the coastal

Downloaded from https://www.cambridge.org/core. 15 Nov 2026 at 21:07:29, subject to the Cambridge Core terms of use.

Dronning Maud Land, East Antarctica. *Journal of the Geological Society of India* **78**(1), 19–29. doi: 10.1007/s12594-011-0063-y.

Thomas ER and Abram NJ (2016) Ice core reconstruction of sea ice change in the Amundsen-Ross Seas since 1702 A.D. *Geophysical Research Letters* **43**(10), 5309–5317. doi: 10.1002/2016GL068130.

Thomas ER and 6 others (2024) The first firn core from Peter I Island – Capturing climate variability across the Bellingshausen Sea. *Climate of the Past* **20**(11), 2525–2538. doi: 10.5194/cp-20-2525-2024.

Thomas ER and 15 others (2017) Regional Antarctic snow accumulation over the past 1000 years. *Climate of the Past* **13**(11), 1491–1513. doi: 10.5194/cp-13-1491-2017.

Turner J and 12 others (2019) The dominant role of extreme precipitation events in Antarctic snowfall variability. *Geophysical Research Letters* **46**(6), 3502–3511. doi: 10.1029/2018GL081517.

Uemura R and 18 others (2018) Asynchrony between Antarctic temperature and CO2 associated with obliquity over the past 720,000 years. *Nature Communications* **9**(1), 961. doi: 10.1038/s41467-018-03328-3.

van Wessem JM and 18 others (2018) Modelling the climate and surface mass balance of polar ice sheets using RACMO2 – Part 2: Antarctica (1979–2016). *The Cryosphere* **12**(4), 1479–1498. doi: 10.5194/tc-12-1479-2018.

Vance TR and 15 others (2024) An annually resolved chronology for the Mount Brown South ice cores, East Antarctica. *Climate of the Past* **20**(4), 969–990. doi: 10.5194/cp-20-969-2024.

Vance TR and 11 others (2016) Optimal site selection for a high-resolution ice core record in East Antarctica. *Climate of the Past* **12**(3), 595–610. doi: 10.5194/cp-12-595-2016.

Velicogna I and 10 others (2020) Continuity of soss in Greenland and Antarctica From the GRACE and GRACE follow-on missions. *Geophysical Research Letters* **47**(8), e2020GL087291. doi: 10.1029/2020GL087291.

Verboncoeur H and 7 others (2025) Multi-decadal evolution of Crary Ice Rise region, West Antarctica, amid modern ice-stream deceleration. *Journal of Glaciology* **71**, e3. doi: 10.1017/jog.2024.79.

Wang W, Shen Y, Chen Q, Wang F and Yu Y (2025) Spatiotemporal mass change rate analysis from 2002 to 2023 over the Antarctic Ice Sheet and four glacier basins in Wilkes-Queen Mary Land. *Science China Earth Sciences* **68**(4), 1086–1099. doi: 10.1007/s11430-024-1517-1.

Wang Y and Xiao C (2023) An increase in the Antarctic surface mass balance during the past three centuries, dampening global sea level rise. *Journal of Climate* **36**(23), 8127–8138. doi: 10.1175/JCLI-D-22-0747.1.

Wauthy S and Dalaiden Q (2026) Role of precipitation and extreme precipitation events on the variability of ice core surface mass balances in Dronning Maud Land: Insights from RACMO2.3 and statistical downscaling. *The Cryosphere* **20**(2), 1279–1296. doi: 10.5194/tc-20-1279-2026.

Wauthy S and 7 others (2024) Spatial and temporal variability of environmental proxies from the top 120 m of two ice cores in Dronning Maud Land (East Antarctica). *Earth System Science Data* **16**(1), 35–58. doi: 10.5194/essd-16-35-2024.

Winstrup M and 19 others (2019) A 2700-year annual timescale and accumulation history for an ice core from Roosevelt Island, West Antarctica. *Climate of the Past* **15**(2), 751–779. doi: 10.5194/cp-15-751-2019.

Winton VHL, Mulvaney R, Savarino J, Clem KR and Frey MM (2024) Drivers of late Holocene ice core chemistry in Dronning Maud Land: The context for the ISOL-ICE project. *Climate of the Past* **20**(5), 1213–1232. doi: 10.5194/cp-20-1213-2024.

Wu T and 19 others (2014) An overview of BCC climate system model development and application for climate change studies. *Journal of Meteorological Research* **28**(1), 34–56. doi: 10.1007/s13351-014-3041-7.

Zuhr AM and 7 others (2026) Airborne radar reveals area-wide decadal increase of sce on the Plateau in Dronning Maud Land, East Antarctica. *Geophysical Research Letters* **53**(8), e2025GL118985. doi: 10.1029/2025GL118985.

Zwally HJ, Giovinetto MB, Beckley MA and Saba JL (2012). Antarctic and Greenland Drainage Systems. *GSFC Cryospheric Sciences Laboratory*. Available at http://icesat4.gsfc.nasa.gov/cryo_data/ant_grn_drainage_systems.php (accessed 10 August 2025).

Downloaded from https://www.cambridge.org/core. 15 Nov 2026 at 21:07:29, subject to the Cambridge Core terms of use.